Weathering processes in the Ganges–Brahmaputra basin and the riverine alkalinity budget

Albert Galy, Christian France-Lanord

▶ **To cite this version:**

Albert Galy, Christian France-Lanord. Weathering processes in the Ganges–Brahmaputra basin and the riverine alkalinity budget. Chemical Geology, 1999, 159 (1-4), pp.31-60. 10.1016/s0009-2541(99)00033-9 . hal-03402710

HAL Id: hal-03402710

https://hal.univ-lorraine.fr/hal-03402710

Submitted on 27 Oct 2021

HAL is a multi-disciplinary open access archive for the deposit and dissemination of scientific research documents, whether they are published or not. The documents may come from teaching and research institutions in France or abroad, or from public or private research centers.

L'archive ouverte pluridisciplinaire **HAL**, est destinée au dépôt et à la diffusion de documents scientifiques de niveau recherche, publiés ou non, émanant des établissements d'enseignement et de recherche français ou étrangers, des laboratoires publics ou privés.

Weathering Processes in the Ganges-Brahmaputra basin and the riverine alkalinity budget.

Albert Galy and Christian France-Lanord

Centre de Recherches Petrographiques et Geochimiques - CNRS, BP 20,54501 Vandceuvre-les-Nancy, France

Corresponding author agaly@crpg.cnrs-nancy.fr

Galy A. and France-Lanord C. (1999) Weathering processes in the Ganges–Brahmaputra basin and the riverine alkalinity budget. Chemical Geology 159, 31–60.

doi: 10.1016/s0009-2541(99)00033-9

Abstract

We present river chemistry data for a network of rivers draining the western and central Nepal Himalaya. Our sampling locations cover the system from the sources of rivers in Tibet to the Gangetic plain. Water samples were collected throughout the year, including the monsoon season, for rivers in Nepal and for the Ganges and Brahmaputra in Bangladesh.

Rivers draining the North Himalaya are characterized by low discharge under a cold and arid climate. Main stream waters have $\delta^{13}C_{DIC}$ near 0 ‰ and high $[SO_4^{2-}]/([SO_4^{2-}]+[HCO_3^-])$ ratios (X_{SO_4}) with values around 40 Eq% and high $[Cl^-]$. Ca is the dominant cation ($Ca^{2+}/\sum$cations = 55 to 75 Eq%, after correction of sodium by chloride). Dissolved sulfate is produced in waters from the TSS whereas chlorine is related to thermal waters. Dissolved sulfate is primarily derived from sulfide oxidation rather than evaporite dissolution. $\delta^{13}C_{DIC}$ values of up to 3.9 ‰ show that metamorphic CO_2 is an important weathering agent. Rivers of the North Himalayan basins have about 50% of their alkalinity derived from carbonate dissolution, 20% from biogenic activity and 30% from metamorphic CO_2.

On the south flank of the Himalaya, rivers are more depleted in ^{13}C and have, on average, lower X_{SO_4}. Most rivers have $\delta^{13}C_{DIC}$ and X_{SO_4} values compatible with a simple mixing between soil CO_2 and sulfate derived from sulfide oxidation. During the monsoon, discharge increases by a factor 20 but the total dissolved concentration is only slightly reduced. X_{SO_4} and $\delta^{13}C$ decrease while Ca/$\sum$cations increases, implying enhanced dissolution of pedogenic calcite.

As a whole, the G-B riverine flux of alkalinity derived from silicate weathering is around 2.7×10^{11} mol/yr, modest at the global scale. Sulphuric acid controls 20-30% of the weathering reaction in the Brahmaputra and 6 to 9% in the Ganges. Na^+ and K^+ balance 60 to 65% of the silicate-derived alkalinity flux, and the long term CO_2 consumption by Ganges and Brahmaputra is near 6.4×10^{10} mol/yr. The flux of metamorphic CO_2 converted to alkalinity via weathering reactions is ca. 1×10^{10} mol/yr.

Keywords

Weathering, Himalaya, Alkalinity, Sulfide, Atmospheric CO_2, Metamorphic CO_2.

1. Introduction

Dissolved fluxes derived from Himalayan erosion and transported to the ocean by the Ganges and Brahmaputra (G-B) rivers exert a strong influence on the chemical budget of some elements at the global scale (Richter et al., 1992; Krishnaswami et al., 1992; Palmer and Edmond, 1992; Derry and France-Lanord, 1996). Several studies have discussed the effect of silicate weathering of the Himalaya on the global uptake of atmospheric CO_2 since the Miocene (e.g. Raymo and Ruddiman, 1992; Goddéris and François, 1996; France-Lanord and Derry, 1997). While there is no doubt that the G-B has a significant impact on the Sr isotope budget of the ocean, the relationship between Sr isotopic fluxes and silicate weathering remains debated (e.g. Quade et al., 1997; Mc Cauley, and De Paolo 1997; Singh et al., 1998). The evaluation of these processes, particularly of the CO_2 uptake by silicate weathering, requires the characterization of the dissolved load of the G-B with regard to its origin (carbonate, silicate or evaporite) and the type of weathering agent involved. Pioneer studies on the G-B chemistry have shown the predominance of carbonate dissolution over silicate weathering and a relative variability of the riverine chemistry from the Himalayan headwaters down to the flood plain (Handa, 1972; Sarin and Krishnaswami 1984; Sarin et al. 1989). From available data on Himalayan rivers, some typical features can be underlined from north to south (Sarin et al., 1989; Sarin et al., 1992; France-Lanord et al. 1995). Headwaters are characterized by high total dissolved solids (TDS) around 350 mg/l, with high ratios of $SO_4^{2-}/\sum$anion . Rivers originating on the southern flank of the Himalaya deliver variable fluxes of dissolved elements, depending on the lithology of their basin. In the flood plain, silicate weathering reactions and tributaries from the south (India) play an important role. Despite these detailed studies, uncertainties remain on the budget of both anions and cations in the G-B, and thus on the budget of silicate alkalinity. In the G-B, 10 to 15% of the anion charge is sulfate that can be derived from either evaporite dissolution or sulfide oxidation. It is necessary to determine if sulfide oxidation is a significant weathering agent in this system or if the high sulfate values represent only "passive" dissolution of evaporitic units. The chemical difference between eroded sediments and their Himalayan source rocks suggests that silicate alkalinity is primarily in the form of alkali cations, which have a significantly smaller impact on net CO_2 consumption than Ca-Mg cations (France-Lanord and Derry, 1997). In order to quantify CO_2 consumption by weathering of the Himalaya, the sources of sulfate and of base cations must be quantified.

In this study, we characterize the weathering reactions in the different zones of the G-B basin and the origin of the dissolved load in order to refine the budget of silicate weathering in the Himalayan system. The study is based on the chemical analyses of

stream waters in different locations of the Narayani basin in Nepal Himalaya, and of the G-B in Bangladesh. Special attention has been paid to the seasonal variability of the riverine chemistry, since most of the dissolved flux is delivered during the monsoon. The data base, including major cations and anions and the isotopic composition of dissolved inorganic carbon, helps to constrain the source of carbonic acid involved in the weathering reactions. In addition, the chemistry of precipitation, the geology of the basin, the mineralogy of the bedload and hydrological data are used to refine this budget of Himalayan chemical erosion.

2. Hydrology and Geology of the Ganges-Brahmaputra basin

The Ganges-Brahmaputra (G-B) basin drains a surface of ca. 1.66×10^6 km^2 in India, Tibet, Nepal, Buthan and Bangladesh (Fig. 1). Four domains can be defined: the G-B plain, the hills and plateau of India to the south of the G-B plain, the Himalaya, and the southern part of the Tibetan plateau. The discharges of the Ganges and Brahmaputra are 459 and 612×10^8 m^3/yr, respectively (GRDC, 1994). A sharp climatic contrast exists between Tibet and the rest of the basin. The southern flank of the range and the plain are exposed to monsoonal precipitation (1 to 4 m/yr) whereas, to the north of the high range, the Tibetan climate is cold and arid with precipitation around 0.2-0.5 m/yr. While the respective area proportions for the G-B plain, southern hills, Himalaya and Tibet are 46:20:18:16, the proportions of annual discharge are 32:9:52:7. This reflects the heterogeneous distribution of precipitation over the basin and the dominant role of the Himalaya in collecting precipitation by orographic effect. Following the major geographical limits, the geology of the Himalaya can be divided into four units separated by major thrust systems. The terranes of the southern part of the Tibetan plateau mostly belong to the Tethian Sedimentary Series (TSS), composed primarily of Palaeozoic-Mesozoic carbonate and clastic sediments (North Indian shelf sediments). Underlying the TSS, the High Himalaya Crystalline (HHC) is the principal formation of the high range. It consists of ortho- and paragneisses, migmatites and highly metamorphosed marbles (Gansser, 1964; Colchen et al., 1986; Le Fort, 1989). The Lesser Himalaya (LH) is composed of variably metamorphosed Precambrian sediments. The lithologies are quartzo-pelitic schists, quartzites, and dolomitic carbonates. The southernmost part of the range consists of the recently uplifted Siwaliks, formed of Mio-Pliocene detrital sediments accumulated in the former Gangetic plain.

3. Sampling and analyses

Water samples were collected in the Narayani watershed, which is one of the four main rivers draining Nepal (Fig. 1 & 2). Sampling includes (1) main tributaries of the Nayarani in the Lesser Himalaya (Kali Gandaki, Marsyandi, Bhuri Gandaki and Trisuli), (2) detailed sampling of the Kali Gandaki from the northern headwaters in the Mustang graben to the south, and (3) minor tributaries of various locations within the basin. Additional basins have been sampled in western Nepal (Karnali, Bheri and Rapti rivers), in Sikkim (Tista river), and some draining the Siwaliks. Samples were collected between May 1993 and April 1997 (Tables 1 to 5), mainly during the dry season, except for the Trisuli and the Bheri rivers which have been sampled repeatedly over one year. The Ganges and Brahmaputra were sampled at different points in Bangladesh during the 1996 monsoon and in winter of 1997 (Fig 1 and Table 5). In Bangladesh we also collected water from the Tista which flows directly from the Himalaya and the Upper Meghna which flows from the Shillong plateau.

All samples were collected from the river bank, filtered through 0.2 μm or 0.1 μm nylon Millipore filters and stored in 2 bottles free of air. One bottle of water was acidified by adding one drop of strong distilled HNO_3. When reported, pH values were determined in the field. Alkalinity was measured by HCl titration in the field for some samples and was always within 7% of the HCO_3^- determined by charge balance.

The $\delta^{13}C$ of dissolved inorganic carbon ($\delta^{13}C_{DIC}$) were measured on CO_2 released by acidification with >100 % H_3PO_4 in vacuum. The sample bottles were opened under an N_2 atmosphere in a glove box and aliquots of 15 to 20 ml were transferred into the reaction vessel. The acidification will release carbonate for highly saline water but no precipitate has been observed in bottles for river waters. The CO_2 released after acidification was extracted while water was trapped as ice at -80°C. Total CO_2 released was measured manometricaly and analysed for $^{13}C/^{12}C$ ratio using a modified VG 602D isotope ratio mass spectrometer. Overall reproducibility is ± 0.2 ‰ for $\delta^{13}C_{DIC}$.

Major element concentrations were measured by ion chromatography at the CRPG. Separation of F^-, Cl^-, NO_3^- and SO_4^{2-} was carried out on a AS12A column using non-acidified water. Acidified water was passed through a CS10 column in order to analyse Na^+, K^+, Mg^{2+} and Ca^{2+}. Each ion was calibrated in a range from 0 to 2 mg/l and the water samples were diluted to fit this range. The detection limit for F^- is 2 ppb, for NO_3^- is 10 ppb and for all other ions, the measured amounts are well above their detection limits. Reproducibility is around 10% (relative) for all ions. HCO_3^- was determined by charge balance from the other ions. Silica was measured by spectrophotometric measurement of the Mo blue complex and 22 samples were duplicated by atomic absorption. These two methods gave comparable results, ruling out the occurrence of significant Si in colloidal form.

4. Results

The data from the Central Nepal basin are presented in Tables 1, 2, and 3 for the Kali Gandaki, Trisuli and other rivers, respectively (Fig. 2). For convenience, the samples have been listed in the tables from north to south. Data from the Western Nepal basins and Siwaliks are listed in table 4. Data from river samples in Bangladesh are given in table 5.

Chemical compositions of Himalayan rivers are highly variable, with total dissolved solid (TDS) ranging from 6 to 880 mg/l. Both the location in the basin and the lithology of the drainage appears to control their chemical characteristics. These are listed in table 6 following the main geographic divisions. All river waters have high relative $[Ca^{2+}]$, with Ca^{2+} representing more than 50 %eq of the total cation charge ($\sum^+$) (Fig 3a). Rivers draining dominantly gneissic terranes in the south flank, some Siwaliks rivers, and basins with a large evaporite component, such as the higher Kali Gandaki, have $[Na^+]$ over 30 %eq of the total cation charge. Overall, rivers draining North flank basins have the highest concentration and are characterized by high relative $[SO_4^{2-}]$ and locally high $[Cl^-]$ (Fig 3b). pH values are always high, between 7.5 and 9.3. With the exception of rivers from gneissic drainage, river waters are always saturated with respect to calcite. This is consistent with the fact that rivers carry 5 to 40% detrital carbonates in the bedload and suspended load. Dissolved inorganic carbon (DIC) has $\delta^{13}C_{DIC}$ ranging between ca. 0‰ in the north to -12 ‰ in Bangladesh. For most samples, pCO_2 concentrations are 5 to 25% higher than calculated or measured $[HCO_3^-]$, implying that waters are significantly supersaturated with respect to atmosphere for dissolved CO_2. The supersaturation reflects equilibration of these waters in a high pCO_2 environment, such as soils or ground water.

The Kali Gandaki has its source in Tibet and descends to the Gangetic plain (Fig. 4). All major Himalayan rivers follow a similar profile (Seeber and Gornitz, 1983), but unlike other major rivers, the upper part of the Kali Gandaki lies in the Mustang graben (one of the Tibetan Neogene grabens). The north basin is characterized by low precipitation (25 to 50 cm/yr), high TDS, and the highest values of Cl^- and SO_4^{2-} in the whole river system. $[Cl^-]$ and $[SO_4^{2-}]$ are however independent as water from the TSS never have high $[Cl^-]$ (< 20 μmol/l). It is only in the graben filling conglomerate that waters have high $[Cl^-]$. Dissolved inorganic carbon is characterized by extremely high $\delta^{13}C$ around 0 ‰ in the main stream of the Kali Gandaki and up to +3.9 ‰ for some tributaries. Cations are dominated by Ca^{2+}, which remains the dominant cation all along the river course. When crossing the high range, precipitation increases very rapidly to reach ≈ 2 m/yr. Despite this increased runoff, TDS remain high, indicating an increase of

the chemical denudation rate on the southern slope of the range. $\delta^{13}C_{DIC}$ decreases gradually as a response to the contribution of the south flank tributaries which have $\delta^{13}C_{DIC}$ around -8 ‰. In the south, the Kali Gandaki is characterized by high relative Cl^- and SO_4^{2-} contents, if compared to most other rivers. These characteristics clearly reflect the contribution of the headwaters in Mustang.

5. Discussion

5.1 Atmospheric input and anthropogenic effects.

The rain water contribution has been estimated from our new and published analyses of rain waters listed in table 7. While the chemistry of rainwater is highly variable, the elemental ratios imply that its chemistry is derived from sea water aerosols as well as from dissolution of continental dust. Excess Ca^{2+} and Mg^{2+} are related to input of terrestrial carbonate and sulfate dust which dissolve in rain water (Sequeira and Kelkar, 1978; Wake et al., 1993). The Cl/Na ratio is lower than that of sea water as well as of oceanic aerosols (Tsunogai et al., 1972) and implies a terrestrial silicate dust contribution for Na as well. Atmospheric inputs are more important close to the Ganges delta than in Himalaya. The Ca/Na and Mg/Na ratios are lower in the plain than in the mountain implying an increase of the dust contribution away from the sea.

Estimates of cyclic salt contribution also imply that evapotranspiration is taken into account. In Nepal, both direct measurement (Alford, 1992) and calculated potential evapotranspiration imply that ca. 25% of the precipitation is affected. In the Ganges plain, evapotranspiration is more important and likely reaches 50% of the precipitation (e.g. Krishnamurthy and Bhattacharya, 1991). On this basis, we estimate the rain water contribution to the riverine dissolved load from the average rain water concentrations multiplied by 1.33 for 25% evapotranspiration in the Himalaya and 2 for 50% evapotranspiration in the Gangetic plain. For rivers in Bangladesh we used a composite of 50% Himalaya rainwater and 50% plain rainwater. The proportion of atmospheric input is about 1 to 10 % of the TDS, except for some high altitude small catchments in the HHC where it can reach 65%.

Anthropogenic activity can modify the chemical signature of river water. In Nepal, Collins and Jenkins (1996) have shown that catchments in agricultural zones are enriched in nitrate and sulfate by 5 to 10 μmol/l over similar forested catchments. This is likely due to the use of N- and K-fertilizers. Some of high altitude rivers (Mailung, Tadi, Hundi), or those with little forested watersheds (Mustang area along the Kali Gandaki

and the Bheri at Dunai) have significant concentrations of nitrate which may reflect the influence of livestock. For all other rivers this contribution remains minor.

5.2 Weathering processes :

5.2.1 Acid involved

One of the unknown in the alteration process is the source of the acid involved in the reaction. Weathering reactions can involve acids from the following sources:

(1) Atmospheric CO_2 dissolved in surface water. In carbonate catchments, it has been shown that kinetic limitations occur during dissolution of carbonate by atmospheric CO_2 leading to maximum [HCO_3^-] around 150-200 μmol/l (Fairchild et al, 1994). This reaction will provide $\delta^{13}C_{DIC}$ around -2 to +2 ‰.

(2) Soil CO_2. Biologic activity in soil enhances pCO_2 far above the atmospheric levels. HCO_3^- in equilibrium with CO_2 produced by degradation of C3 plant should have a $\delta^{13}C$ around -18‰. A silicate weathering reaction consuming soil CO_2 should then produce HCO_3^- at -18‰, whereas carbonate dissolution should release HCO_3^- at -9‰, because half of the HCO_3^- is derived from the carbonate.

(3) Metamorphic CO_2. We sampled thermal springs highly enriched in ^{13}C at five locations in the Mustang graben at the contact between the graben-filling conglomerate and the basement formations. These springs are always characterized by $\delta^{13}C$ above +10‰, [HCO_3^-] between 6000 and 120 000 μmol/l, variable [Cl^-] and [SO_4^{2-}], and are associated with CO_2 degassing. The production of dry CO_2 at depth by metamorphic decarbonatation around 300-400°C creates gas enriched in ^{13}C by 2 to 6‰ with regard to the original rock (Shieh and Taylor, 1969; Friedman and O'Neil, 1977). The evolved CO_2 is further dissolved in ground water that produces HCO_3^- having a $\delta^{13}C$ 6-10‰ higher than that of the gas (Mook et al., 1974). A contribution of this type of alkalinity is clear in the Narsing river with $\delta^{13}C$ = +3.9 ‰ requiring a source of enriched CO_2. One spring water which flows into this river has been analysed with [HCO_3^-] around 30 000 μmol/l and $\delta^{13}C_{DIC}$ = + 13.5 ‰.

(4) Sulfuric acid derived from sulfide oxidation. Sulfuric acid will react with calcite and silicate. The HCO_3^- released by this reaction have the $\delta^{13}C$ around zero permil.

The characteristic and contribution of acids to the weathering budget can be estimated using $\delta^{13}C_{DIC}$, which varies with the source of the carbonic acid, and the sulfate proportion (X_{SO_4} eq%). The proportion of carbonate/silicate altered and of the four

weathering acids provide the covariations of X_{SO_4} with $\delta^{13}C_{DIC}$ shown in figure 5. The alkalinity budget and X_{SO_4} can be described by the 3 equations:

$[HCO_3^-]_{tot} = [HCO_3^-]_{carb} + [HCO_3^-]_{bio} + [HCO_3^-]_{meta} + [HCO_3^-]_{atm}$

$\delta^{13}C_{tot} = (\sum_i [HCO_3^-]_i \times \delta^{13}C_i) / [HCO_3^-]_{tot}$

$X_{SO_4} = ([SO_4^{2-}]_{sulfide} + [SO_4^{2-}]_{evaporite}) / ([SO_4^{2-}]_{tot} + [HCO_3^-]_{tot})$

where total alkalinity is the sum of HCO_3^- derived from *i* inputs: carbonate dissolution (carb), biologic (bio), metamorphic (meta) and atmospheric (atm). This system can be simplified assuming that : (1) direct weathering by atmospheric CO_2 is negligible, (2) sulfuric and carbonic acids alter carbonate and silicate without any selectivity, (3) $[HCO_3^-]_{carb} = [Ca^{2+}]-[Na^{+*}] \times 0.2$ (see appendix). In the case of weathering without metamorphic CO_2, compositions plot on the curves drown on figure 5 for different proportion of carbonate to silicate altered. For the end member case where all weathering is produced by reaction with H_2SO_4, X_{SO_4} vary between 0.5 for dissolution of carbonate and 1 for silicate (Fig. 5).

5.2.2 Mustang basin - Kali Gandaki headwaters

Main stream Kali Gandaki waters are characterized by high $\delta^{13}C_{DIC}$ (close to 0‰), high sulfate content around 40 eq%, high chlorine content around 10 eq%, and dominant proportion of Ca in the cations ($X_{Ca} = Ca^{2+}/\sum$cations of 55 to 75 eq%, after correction of sodium by chloride). Waters are always over saturated with respect to calcite, and detrital carbonate was found in all bedload sands. High $[Cl^-]$ are restricted to catchment draining the conglomerate formations which fill the Mustang graben. Surrounding tributaries draining the TSS formations have low $[Cl^-]$. Therefore, Cl^- is likely derived from thermal spring circulations enriched in Cl^- and/or from the leaching of salted lenses described in the basal formation of the conglomerate (Tshering and Bhandari, 1973 in Fort, 1996).

Except in the extreme north, Mustang river waters have high sulfate contents. Sulfate can be derived from either dissolution of $CaSO_4$ minerals in sedimentary evaporites or from oxidation of sulfide minerals. Both source are possible in the Mustang context since (1) high $[Cl^-]$ imply that evaporitic material is altered and (2) pyrite is present in the Mesozoic formations of the TSS (Bordet et al 1971). Saline waters in glacial environments are frequently associated to this last reaction (Vennum, 1980; Chillrud et al., 1994; Fairchild et al, 1994; Williams et al., 1995). The evaporitic origin is not supported by the lack of correlation between $[Cl^-]$ and $[SO_4^{2-}]$. Sulfate is released in the TSS waters whereas chloride concentrations remain low. The most extreme example is NAG24 (table 3) which is glacial water flowing on TSS terrain and contains

only 4 μmol/l Cl^- for 2852 μmol/l of SO_4^{2-}. For these reasons we argue that the dissolved sulfate mostly derives from sulfide oxidation.

$\delta^{13}C_{DIC}$ are high in almost all Mustang waters which is not common in rivers (e.g. review in Mook and Tan, 1991). $\delta^{13}C \approx 0‰$ could be reached via several scenarios. CO_2 equilibration with the atmosphere is unlikely because these rivers are significantly supersaturated in CO_2 with respect to atmosphere. Degassing of CO_2 tends to increase the $\delta^{13}C$ of remaining DIC, but such degassing will only increase the $\delta^{13}C_{DIC}$ by about 0.5‰. Photosynthetic activity tends to increase $\delta^{13}C_{DIC}$ (Pawellec and Veizer, 1995) but is not important in the cold and arid climate of this basin. Carbonate dissolution promoted by dissolved atmospheric CO_2 will deliver DIC around 0‰ but these reactions cannot account for the high CO_2 concentrations measured in these waters. Finally, the weathering of carbonate by sulfuric acid delivers DIC around 0‰. Given the X_{Ca} of these rivers, the X_{SO_4} ratio should be between 0.65 and 0.80 if sulfuric acid was the only weathering agent or even higher if some SO_4^{2-} is derived from evaporite. Our data are lower around 0.5 and imply that carbonic acid also contributes to weathering reactions (Fig. 6a). In figure 6a, all samples lie to the right of the mixing trend between the H_2SO_4 and the "Biological" CO_2. A contribution of metamorphic CO_2 could satisfy the carbon isotopic budget. To the extreme north, $[SO_4^{2-}]$ are low and samples of the main stream of the Kali Gandaki (LO 49) have variable $\delta^{13}C_{DIC}$ (-3.2 and +1.3 ‰) and $[Cl^-]$ (270 and 930 μmol/l). One minor local tributary (LO 25) has lower $\delta^{13}C_{DIC}$ at -6.7‰ and low $[Cl^-]$, reflecting a greater influence of soil weathering reactions. On the other hand, nearby spring waters have very high $[Cl^-]$ (93000 μmol/l) and $\delta^{13}C_{DIC}$ around +10‰, with $[HCO_3^-]$ of 36800 μmol/l. The two samples of the Kali Gandaki are consistent with mixing between spring waters enriched in metamorphic CO_2 and surface water enriched in biologically derived CO_2 (represented by sample LO 25). Downstream, the chemistry of the Kali Gandaki becomes strongly enriched in sulfate while its $\delta^{13}C_{DIC}$ varies little between -1.4 and 0.4 ‰ (Fig. 6a). These chemical signatures indicate the contribution of a tributary where sulfide oxidation and metamorphic CO_2 are important weathering agents, such as in sample LO 96.

Following the simplifications of the alkalinity budget (section 5.2), we find that about 50% of the alkalinity is derived from carbonate dissolution, 20% from biogenic CO_2, and 30% from metamorphic CO_2. This rough budget underlines the importance of metamorphic CO_2 in the chemical budget of these rivers.

The Kali Gandaki headwaters are characterized by the role of sulfide oxidation and metamorphic CO_2 as weathering agents. The importance of sulfuric acid could be a relatively general feature of the north flank basins because most rivers flowing from the north Himalaya have high $[SO_4^{2-}]$. In Nepal, the Bhote Kosi, Marsyandi, Seti, and

Bheri in their upper reaches have high $[SO_4^{2-}]$. In the Garhwal Himalaya, high $[SO_4^{2-}]$ in river water or in melt waters were also proposed to partially result from oxidation of pyrite (Sarin et al., 1992; Hasnain and Thayyen, 1996). We have no data which permit us to evaluate the importance of metamorphic CO_2 as a weathering agent in these north Himalayan basins. The metamorphic CO_2 is restricted to the graben of the Thakkhola in the Kali Gandaki, but this type of heavy dissolved carbon was also suggested for the Tibetan lakes (Fontes et al., 1996) and may represent a general feature for catchment linked to major tectonic depression.

5.2.3 South flank rivers

When crossing the high Himalaya, large rivers like the Kali Gandaki have decreasing $\delta^{13}C_{DIC}$ (Fig. 4). This is due to progressive contribution of south flank catchments, where two types of rivers can be defined on the basis of the lithology of their basin . Rivers flowing in carbonate-free basin have low TDS, around 15 to 50 mg/l, and lower X_{Ca}. In these rivers the cyclic contribution is important and may represents up to 50% of the dissolved load. For this reason, we will use data corrected for cyclic contribution (marked by an asterisk) in the following discussion. Basin with carbonate units from the TSS, HHC or LH have higher TDS (100 to 270 mg/l) linked to a higher X_{Ca}. In both river types, the X_{SO_4} ratio is variable, between 0.05 and 0.35, even after correction for cyclic sulfate. Altogether, these rivers have lower $\delta^{13}C_{DIC}$ than the north flank rivers, implying that biologically derived alkalinity becomes more important. This is consistent with the higher proportion of forested area on the south flank of the Himalaya. The $\delta^{13}C_{DIC}$ varies from -12 to -3‰ and tends to increase with sulfate in the dissolved load. In the $\delta^{13}C_{DIC}$ - X_{SO_4} space, most samples are compatible with a model of alteration driven by both H_2SO_4 and biologically derived HCO_3^-. No anhydrite or gypsum has been described in the HHC or LH, whereas sulfides are present in all these formations. In the south flank catchments of Kumaun Himalaya (Bartarya, 1993), some formations of the LH contain pyrite that was suggested to be the source of sulfate (around 300 μmol/l) in river water, while $[Cl^-]$ remained low (65 μmol/l). Hence, as for the north Himalayan basins, sulfide dissolution appears to be the most likely source of dissolved sulfate in river water.

The alkalinity budget is certainly more complex than a simple mixing between biologically derived HCO_3^- and H_2SO_4. The $\delta^{13}C$ of the biological HCO_3^-, chosen at -18‰, is likely to be different for the high altitude samples where soils are poorly developed and for the LH samples where thick soils are developed under dense mixed jungle. However, some high altitude stream samples have low $\delta^{13}C_{DIC}$ (-9.5 to -8.5‰).

This shows that, even where soil is poorly developed, the biological activity enhances pCO_2 and thus weathering reactions. Second, the $\delta^{13}C$ of carbonate rocks is variable from +1‰ in the TSS to -2‰ in the LH (Galy et al., submit). In addition, metamorphic CO_2 may contribute to the alkalinity. This is likely the case for NH 39 that has been sampled near the MCT, very close to the hot springs (Tatopani) of the Seti khola. Two samples of these hot springs have a $\delta^{13}C_{DIC}$ of +3.7 and +2.1‰. The Langtang khola (LO 257 and NH 100) was also sampled near hot springs in Shyabrubensi which have high $[HCO_3^-]$ and $\delta^{13}C$. However, most hot springs from the south flank have low $\delta^{13}C_{DIC}$ and the influence of hot spring waters on south flank rivers is probably only local.

5.2.4 Main rivers and annual variability

Main Himalayan rivers sampled in the LH have chemical characteristics inherited from the contribution of the different basins. The range of variation of $\delta^{13}C_{DIC}$ and X_{SO_4} remains very large (-13 to -4‰ and 0.07 to 0.22, respectively. Fig. 6b). It is tempting to relate the values observed for the different main rivers to the characteristics of their drainage. For instance, the lower Kali Gandaki samples have all high X_{SO_4} reflecting the contribution of its upper basin. However, the seasonal variability of the chemical signature at a given location is large and most of our sampling locations have been sampled only once. The sampling of the Trisuli river at Betrawati over one year has a chemical variability which overlaps almost entirely the range of variation of the major Himalayan rivers (Fig. 6b).

The Trisuli river at Betrawati shows systematic trends during and belong the monsoon season (Fig. 7). The onset of the monsoon is marked by a 20% increase in TDS, despite river discharge increases by a factor 10. This is the result of an increased input of HCO_3^- and Ca^{2+}, whereas $[SO_4^{2-}]$, $[Na^+]$, $[Mg^{2+}]$, and [Si] decrease over the same period. This trend is reversed after mid July until the end of the monsoon. Afterward, TDS increases together with X_{SO_4} and X_{Na}, and $[Ca^{2+}]$ concentrations become positively correlated to $[Mg^{2+}]$. These variations imply two distinct trends during and outside the monsoon (Fig. 8). During the monsoon, the variation is essentially driven by the input of Ca^{2+} and HCO_3^- which reach a maximum around mid July.

Swelling processes imply that ground water in the sub-surface aquifer are flushed out during the early rains. The average chemistry of ground water is difficult to estimate but March-April river chemistry may be a proxy as the proportion of aquifer is high during the dry period. Therefore the hystheresis process at the beginning of the monsoon

will show and increase of the TDS correlated with the rise the X_{SO_4}. This can be the case in May, when the first precipitation reach the range (Climatological records of Nepal). However the chemical evolution of the Trisuli in July (Fig. 7 & 8) can not be the result of swelling processes.

One possible source of this trend is the input of $CaCO_3$ rich rain water in the system at the beginning of the monsoon. Himalayan rain water can have Ca^{2+} concentrations as high as 100 to 300 μmol/l, probably due to dust input from central Asia (Wake et al., 1990). Precipitation with high $[Ca^{2+}]$ could explain the observed trend during the monsoon, however it is likely that precipitation would have a $\delta^{13}C_{DIC}$ near 0‰, whereas Trisuli river samples during the monsoon show a decrease in $\delta^{13}C_{DIC}$ toward a minimum of -10‰. The observed increase in $[Ca^{2+}]$ and $[HCO_3^-]$ is therefore more likely due to the dissolution of calcite in the basin. Enhanced detrital calcite dissolution is possible in the river since suspended load concentration reach its maximum in July when it is multiplied by 20 with regard to the dry season average. However, detrital calcite dissolution in the river would raise rather than lower $\delta^{13}C_{DIC}$. Alternatively it is possible that pedogenic calcite formed in soils during the dry season is preferentially dissolved at the beginning of the monsoon. Pedogenic carbonate derived from the respiration of C3 plant material has low $\delta^{13}C$ (Cerling et al., 1989). We do not have data on pedogenic carbonate concentration in soils but the observed trend in the Trisuli water would require dissolution of only 0.01 wt% of calcite assuming leaching of 10 cm thick soils over the whole basin. This hypothesis appears therefore as the most likely. During the dry season, the chemical signature of the Trisuli is very similar to that of its northern tributary, the Bhote kosi. There is no relationship between X_{SO_4} and $\delta^{13}C_{DIC}$ which is likely due to the fact that during the period of low discharge the influence of hot springs with high $\delta^{13}C_{DIC}$ is important.

The trend of calcite dissolution during the monsoon is clearly observed for the Trisuli and the Tista (increasing $Ca^{2+}/\sum$cations, $HCO_3^-/\sum$anions; Table 2 and 5). Other rivers appear to show the same seasonal trend, although less pronounced (Bheri Table 3 and data in Sarin, 1989). The effect of pedogenic carbonate dissolution is more apparent in the Trisuli and the Tista because limestone dissolution does not overprint their chemical signature as strongly as in other basins. The proposed effect of pedogenic carbonate leaching at the beginning of the monsoon may be widespread.

5.2.5 Ganges and Brahmaputra

The Ganges and Brahmaputra sampled in Bangladesh during the monsoon (Table 5) have chemical characteristics very similar to those of the main Himalayan rivers at the outflow of the range. They are also close to the mean annual composition reported by the

GEMS/Water program (UNESCO). During the dry season, the Brahmaputra follows an evolution similar to that of Himalayan rivers, with a slight increase of TDS (105 to 153 mg/l) and an increase of X_{SO_4} and $\delta^{13}C_{DIC}$ (Fig 6b). In contrast, TDS in the Ganges almost triples (125 to 370 mg/l) due to the general increase of ion concentrations, with the notable exception of K^+ and SO_4^{2-}. The observed trend is consistent with data reported by Sarin et al. (1989) for the Gangetic plain. These authors have shown that during the dry season, the influence of southern tributaries and of weathering processes in the flood plain become significant relative to Himalayan input. $\delta^{13}C_{DIC}$ of the Ganges increases by about 2‰ during the dry season, while X_{SO_4} decreases from 0.10 to 0.03 (Fig 6b). It is possible that this trend reflects a change in the isotopic composition of the biologically derived DIC. The Gangetic plain and the southern tributary catchments are in the C4 photosynthetic zone. consequently, the $\delta^{13}C_{DIC}$ in soils should be higher by several ‰ than for the Himalayan soils (e.g. Cerling et al., 1989)

5.3 Silicate to carbonate weathering

5.3.1 Chemical budget

Soluble elements in rivers are a mixture of atmospheric input and weathering of silicate, carbonate, sulfide and evaporite minerals. For any element X we can therefore write the budget equation:

$$[X]_{river} = X_{cyclic}+X_{evaporite}+X_{carbonate}+X_{silicate}+X_{sulfide}+X_{anthropogenic}$$

The mixing relationships of elemental or isotopic ratios can help to identify and quantify the end members and their relative proportions. In order to decipher the relative contribution of the different end members, we apply a forward modelling of the river chemistry, complemented by constraints of geology and the chemistry of stream sediments. Selected small catchments of given lithology define the chemical characteristics for weathering of different rocks units. This allowed to express the silicate to carbonate budget by the ratio X_{sil} and is presented in appendix. The X_{sil} is the ratio of dissolved cations from silicates over the sum of dissolved cations from silicates plus carbonates expressed in eq%.

The main error on this estimate arises from $Mg_{silicate}$ and $Ca_{silicate}$. We can consider that $0.15 < (Ca^*/Na^*)_{sil} < 0.25$ and $0.25 < (Mg^*/K^*)_{sil} < 0.75$ (Fig. 9). When applying these ranges of values, the propagated relative uncertainty on X_{sil} is less than 22%. This upper limit applies to samples with very low X_{sil} values; more typically the uncertainty is 15%. The calculation of X_{sil} is only relevant for catchments that are

large enough to average the chemical heterogeneity of bedrock formations, and have TDS high enough so that cyclic contributions are minor. The silicate to carbonate weathering ratio will therefore be discussed for large basins only.

5.3.2 Spatial variability of X_{Sil}.

If we examine only the major basins, for which the lithology is always mixed, X_{sil} shows systematic variability. The catchments of the north flank rivers are carbonate-rich and correspond to the lowest X_{sil} (0.07 ± 0.02 for the Upper Kali Gandaki). Rivers with large basins in the TSS have low X_{sil} : Kali 0.06 to 0.09; Marsyandi 0.07; Bheri 0.06 to 0.10. The Trisuli or the Tista, which have a small fraction of their catchment areas in the TSS, have high X_{sil} around 0.19 ± 0.03 and 0.31 ± 0.07, respectively.

At the G-B basin scale, the main Himalayan tributaries have variable proportions of carbonate terranes, and X_{sil} varies from 0.10 to 0.31. The Ganges and the Brahmaputra have X_{sil} = 0.18-0.23 and 0.12-0.17, respectively. These values could simply imply that the Brahmaputra basin has more carbonate than the Ganges basin does, in contradiction to the geology of the Himalayan parts of their basins. More likely, the values are a reflection of an higher physical/chemical erosion in the Brahmaputra basin. In the Ganges, the apparent enhanced relative rate of silicate weathering may reflect processes in the Siwaliks basins and in the Ganges flood plain. Rivers draining the Siwaliks are characterized by X_{Sil} between 0.2 and 0.7, the highest in the system (Table 4). For the flood plain, data of Sarin et al.(1989) on the Gomti river, which only drains the plains, and for ground waters have a X_{sil} around 0.35, significantly higher than that of the Ganges. We lack yearly records and sufficient hydrological data to quantify the exact influence of both domains, but it is clear that weathering in the lowlands and in the flood plain tends to increase the ratio of silicate weathering in the Ganges. The observation that the flood plain is an important site for silicate weathering is consistent with the long term record of Himalayan weathering preserved in the Bengal Fan (Derry and France-Lanord, 1996).

5.3.3 Rate of chemical erosion

Chemical erosion can be estimated from our budget of silicate/carbonate weathering and surface and hydrological data available for the basin. This type of approach allows us to compare rates of erosion between different basin where we have sufficient data to estimate yearly discharge. Therefore we present chemical erosion rates only for the Narayani, Trisuli, Bheri, Tista, and G-B (Table 8).

The Trisuli and Bheri annual records exhibit a large increase of both carbonate and silicate chemical erosion with the onset of the monsoon. The silicate chemical erosion rates (SCE) are similar in these basins, while the carbonate chemical erosion rates (CCE) are always 3 to 4 times higher in the Bheri watershed. The Bheri basin is rich in carbonate rocks compared, to the Trisuli and Tista, and the difference in the CCE is likely to result primarily from the lithology of the respective catchments. When the lithology is not the limiting factor for CCE, the chemical erosion is 10 times higher for carbonate than for silicate. The average chemical erosion rate obtained for large Himalayan rivers (Table 8) is similar to that of Andean rivers for silicate (0.007 mm/yr; Gaillardet et al., 1997) but 4 to 5 more important for carbonate. A higher proportion of limestone in the Himalayan terranes is likely to explain this difference.

In Bangladesh, the Brahmaputra shows chemical erosion rates very similar to those of the Tista or Trisuli. This is consistent with the Himalayan character of the river and the relatively low proportion of carbonates in the non-Tibetan part of the watershed. The Ganges displays significantly lower chemical erosion rates, compared to Himalayan rivers, especially for carbonates (Table 8). The chemical flux of the Ganges plain, calculated as the difference between Ganges and the sum of the Himalayan and southern tributaries (Table 9), allows us to estimate SCE and CCE for the flood plain at 0.001 and 0.004 mm/yr respectively. The Gomti river (Subramanian et al., 1987; Sarin et al., 1989), which drains only the central Ganges flood plain, also has low SCE and CCE (0.003 and 0.009 mm/yr, respectively). The very low CCE in the plain may result from the relatively low amount of carbonate available for dissolution. Our analyses of the Ganges bedload in Bangladesh shows that it contains ca. 6 wt% of detrital carbonate. Thus much less carbonate is exposed to dissolution in the flood plain than in the Himalaya. Low SCE and CCE may also result from drier conditions in the plain than in the Himalayan part of the basin. For the entire dry season, the atmospheric water balance is negative in a large part of the plain, which behaves almost as an endoreic system. Such dry conditions are responsible for the development of alkaline soils (Sarin et al., 1989). Over one year, intense evapotranspiration in the plain results in an effective discharge of only 0.4 to 1 m/yr, despite precipitation between 1 and 2 m/yr (Henning, 1989).

The low SCE is however somewhat contradictory with the increase of the smectite and kaolinite proportion in the clay fraction of suspended load along the Ganges course measured by Sarin et al. (1989). This apparent discrepancy may results from a hidden flux of dissolved elements in the system. Based on a study of radium and barium fluxes, Moore (1997) has shown that there is an active submarine discharge of ground water at the G-B mouth. While the magnitude of the water flux is not accurately known it could be between 0.35 to 3.5 time that of the rivers. Since ground waters have higher concentrations of dissolved species than river water, this may imply a notable flux of

dissolved elements. The hydrological budget of the Ganges system supports this hypothesis. The runoff for the Ganges plain calculated from the difference of the Ganges flux at the mouth and the sum of all its major tributaries collected from hydrological data (Rao, 1979; Hossain et al., 1987; Alford, 1992; Dept. of Hydrology and Meteorology, unpub. data) is ca. 0.3 m/yr. Such value is significantly lower than the average discharge (0.4 to 1 m/yr) calculated as the difference between precipitation and evapotranspiration (Henning, 1989). Uncertainties remain, but several independent evidences suggest a possibility of significant ground water flux at the G-B mouth.

5.4 Long term CO_2 atmospheric uptake by the Ganges-Brahmaputra system

The alkalinity flux carried by the G-B rivers corresponds to 3.7% of the world riverine flux to the ocean according to Berner and Berner (1996). This value is higher than the fresh water flux (2.8% of the global) and suggests a high weathering rate in G-B. Lithology is a key parameter controlling weathering rate (Meybeck, 1987), and the ubiquitous occurrence of carbonates from the north flank of the Himalaya in the sands in Bangladesh controls the TDS. With regard to long term CO_2 uptake, only the alkalinity flux linked to silicate weathering is important. For the combined G-B flux, the fraction of cationic charge derived from silicate weathering is ca. 23%. We estimate that ca. 70% of the sulfate flux of the G-B derives from the oxidation of pyrite in the Himalaya (the remaining sulfate being derived from cyclic salts and from Indian shield tributaries). The exact proportion of silicate and carbonate altered by sulphuric acid instead of CO_2 is difficult to estimate, but clearly a significant fraction of the cationic charge derived from silicate alteration is balanced by SO_4^{2-} rather than HCO_3^-, and thus does not contribute to the alkalinity. If all of the sulfide-derived sulfate reacted with silicates, the silicate alkalinity flux would be 1.40×10^{11} mol/yr. If this sulfuric acid reacted only with carbonates, the silicate alkalinity flux would be 2.95×10^{11} mol/yr. Assuming that sulphuric acid weathers carbonate and silicate in the same proportion as the CO_2 does, the silicate alkalinity flux is around 2.66×10^{11} mol/yr.

The silica flux may also be used to estimate the alkalinity flux linked to the silicate weathering (Edmond et al., 1996) while in areas of high physical erosion it may be an underestimate. The G-B silica flux would suggest a silicate alkalinity flux of 2.73×10^{11} mol/y, in the range of our estimates. These estimates would correspond to 2.3% of the global riverine silicate alkalinity flux (Berner and Berner, 1996; Ludwig et al., 1996). Weathering in the G-B basin appears less efficient as a sink of atmospheric CO_2 than in other tropical-equatorial basins, such the Amazon and the Congo (Edmond et al., 1996;

Gaillardet et al, 1995). Additionally, 60 to 65 % of the silicate alkalinity in the G-B is balanced by Na^+ and K^+. This is close to, but slightly lower than, the estimate established from the chemical difference between HHC and eroded sediments (France-Lanord and Derry, 1997). Only a part of Na^+ and K^+ is exchanged for Ca^{2+} in the marine environment, allowing alkalinity to precipitate as carbonate. The rest undergoes reverse weathering reactions which return alkalinity to the atmosphere. The effectiveness of these processes is poorly constrained, but assuming that 20% of K^+ and 30% of Na^+ are exchanged for Ca^{2+} (France-Lanord and Derry, 1997), the modern CO_2 consumption by Ganges and Brahmaputra would be around 6.4×10^{10} mol/yr. Using the same assumptions, the global uptake of atmospheric CO_2 by silicate weathering calculated from river chemical data should be around 48.5×10^{11} mol/yr (Berner and Berner, 1996). Thus, with 1.3% of the global long term CO_2 uptake, the G-B basin appears to be a minor control on atmospheric pCO_2. In the reality, the G-B CO_2 uptake is likely to be higher if the probable flux of ground water to the ocean is taken into account. This flux remains to be accurately estimated. However, the low rate of CO_2 uptake in the G-B basin is, in part, the result of a very low proportion of Ca- and Mg-silicates in Himalaya and this will apply also to the ground water.

6. Conclusion

The G-B river system is remarkable for the diversity of erosion and weathering regimes active in its different parts. From Tibet to the flood plain the influence of the tectonic processes, lithology of eroded terranes, and climate all contribute to the final chemical signature of the G-B waters.

Himalayan tectonic activity affects chemical weathering in several ways. First, the high rate of uplift in the High Himalaya develops steep relief and high elevation surfaces. These terranes are therefore undergoing rapid physical erosion instead of slow processes of soil development. Himalayan tectonics acts in this case as a limiting factor for chemical erosion. Second, in the southern part of Tibet, extentional grabens degas metamorphic CO_2. Dissolved in ground water, this CO_2 is an important source of carbonic acid for weathering in the northern basins. At the G-B scale, their contribution is nevertheless negligible, of the order of 10^{10} mol/yr. Third, development of the foreland basin at the front of the range (e.g. Burbank, 1992) accumulates silty material in the flood plains that favours circulation of the ground water. This region is likely dominated by silicate weathering reactions, such as these observed in the rivers draining the Siwaliks. Flood plain ground water may represent a significant flux toward the

ocean, as proposed by Moore (1997). However, this flux remains to be quantified for major dissolved elements.

The main lithologic parameters are the presence of carbonate, in the TSS, the presence of sulfides, and the composition of silicate rocks. Carbonate units overprint the chemical riverine signature form north to south. Despite the fact that they are mostly exposed in zones of high altitude and low precipitation, carbonates are the main source of dissolved elements. Cations derived from carbonate dissolution represent 80 to 90 % of the total cationic charge in all parts of the basin, except in purely silicate drainage. The presence of sulfide plays an important role as weathering agent. Sulphuric acid derived from sulfide oxidation results in a high rate of weathering in places where low precipitation and temperature do not favour chemical weathering. Overall, sulphuric acid controls 20-30% of the weathering reactions in the Brahmaputra and 6 to 9% in the Ganges. The high level of oxidized sulfide in the G-B is likely accompanied by release of PGE. They therefore represent a potential source of radiogenic Os in the Himalayan erosion as inferred by Pegram et al. (1992). Finally, the dominantly alkaline composition of Himalayan silicate rocks implies that most of the cations released by silicate weathering are Na^+ and K^+. Because these cations exchange incompletely with Ca^{2+} and Mg^{2+} to precipitate carbonate, this reduces the potential uptake of atmospheric CO_2 by Himalayan silicate weathering. Despite a relatively important flux of alkalinity, the overall long term CO_2 uptake related to modern Himalayan erosion appears minor on the global scale.

The climate controls the weathering style and intensity. To the north of the high range, the arid and cold climate does not favour soil development. Weathering reactions are therefore dominated by inorganic processes driven by sulfide oxidation or by carbonic acid derived from metamorphic degassing. We do not have a yearly average of dissolved fluxes for the Upper Kali Gandaki, but the estimated rate of chemical erosion is between 0.02 and 0.05 mm/yr, low for a carbonate rich basin. On the southern flank of the range, heavy rainfall and tropical temperatures enable development of soils and vegetative cover up to 4000 m altitudes. In these basin, weathering reactions are dominantly driven by carbonic acid derived from biologic activity in the soils. Under these conditions, the rate of chemical erosion reaches 0.005 mm/yr for silicates and 0.06 mm/yr for carbonates. In the flood plain, despite heavy monsoonal rainfall, high temperature and favourable physical conditions (flat soils and alluvial material), the rate of chemical erosion appears lower than in the Himalaya. The low rates may result from the atmospheric water balance which is strongly influenced by evapotranspiration, and dry conditions prevail in the plain for large parts of the year. At the G-B scale, differences appear between the two river system. The Brahmaputra basin is exposed to more intense monsoon than the Ganges, as

shown by their respective runoffs of 1090 (Brahmaputra) and 617 mm/yr (Ganges). The rate of chemical erosion for each system are similar, but this is difficult to interpret because the geographic and geologic distribution of surface area in the two basins are very different. More meaningful are (1) the mineralogical composition of the clay fraction in the sediment load with smectite+kaolinite around 20% for Brahmaputra and 60% for Ganges, and (2) the ratio of physical to chemical flux, which is 9.3 for Brahmaputra and 3.9 for the Ganges. These data clearly show that erosion in the Brahmaputra basin is more influenced by physical processes when compared to the Ganges. From this comparison, the monsoonal climate appears to be the limiting factor for weathering as it favours rapid physical erosion and transport.

Acknowledgements

This work would have been impossible without the sampling assistance of number of Himalayan geologists: A. Gajurel, P. Le Fort, J-L. Mugnier, B. Marty, R. Muralt, and the "MO" team. We greatly thank the analytical assistance of P. Coget, O. Gabens, B. Jacquier, E. F. Rose and M. Vernet. We also thank Prof. B.N. Upreti for his constant help during this project in Nepal. The collaboration of M. D. Shafiqul Alam from the department of Archeology of Bangladesh and K. Pedoja under the auspices of "la mission d'Orient" made sampling in Bangladesh possible. This paper has benefited from fruitful discussion with L. A. Derry and P. Le Fort, and from reviews by S. Krishnaswami, M. R. Palmer and J. Veizer. This work was supported by the CNRS-INSU programs DBT "Fleuves et Érosion" and PROSE. A. G. was supported by a CNRS-Région Lorraine grant during this study. CNRS-INSU-DBT contribution # XXXX and CRPG-CNRS contribution # 1340.

References

Alford D., 1992. Hydrological aspects of the Himalayan region. ICIMOD Occasional paper No. 18.

Bartarya S. K., 1993. Hydrochemistry and rock weathering in a sub-tropical Lesser Himalayan river basin in Kumaun, India. Journal of Hydrology, 146: 149-174.

Bäumler, R. and Zech, W. 1994. Soils of the high mountain region of Eastern Nepal: classification, distribution and soil forming processes. Catena, 22: 85-103.

Berner, R. A. and Berner, E., 1996. Global Environment : Water, Air, and Geochemical Cycles. Prentice Hall.

Blum, J. D., Gazis, C. A., Jacobson ,A. D., and Chamberlain, C. P., 1998. Carbonate versus silicate weathering in the Raikhot watershed within the High Himalayan Crystalline Series. Geology, 26: 411-414.

Bordet, P., Colchen, M., Krummenacher, D., Le Fort, P., Mouterde, R. and Remy, M., 1971. Recherches Géologiques dans l'Himalaya du Népal, Région de le Thakkhola. Centre National de la Recherche Scientifique.

Brouand, M., 1989. Pétrogenese des migmatites de la dalle du Tibet (Himalaya du Népal). Ph.D. Thesis, INPL, Nancy, France.

Burbank, D. W., 1992. Causes of recent Himalayan uplift deduced from deposited patterns in the Ganges basin. Nature, 357: 680-683.

Cerling, T. E., Quade, J., Wang, Y. and Bowman, J. R., 1989. Carbon isotopes in soils and palaeosols as ecology and palaeoecology indicators. Nature, 341: 138-139.

Chillrud, S. N., Pedrozo, F. L., Temporetti, P. F., Planas, H. F. and Froelich, P. N., 1994. Chemical weathering of phosphate and germanium in glacial meltwater streams: Effects of subglacial pyrite oxidation. Limnology and Oceanography, 39: 1130-1140.

Colchen, M., Le Fort, P. and Pêcher, A., 1986. Notice explicative de la carte géologique Annapurna-Manaslu-Ganesh (Himalaya du Népal) au 1:200.000e (bilingue: français-english). Centre National de la Recherche Scientifique.

Collins, R. and Jenkins, A., 1996. The impact of agricultural land use on stream chemistry in the Middle Hills of the Himalayas, Nepal. Journal of Hydrology, 185, 71-86.

Derry, L. A. and France-Lanord, C., 1996. Neogene Himalayan weathering history and river $^{87}Sr/^{86}Sr$: Impact on the marine Sr record. Earth and Planetary Science Letters, 142: 59-74.

Edmond, J. M., Palmer, M. R., Measures, C. I., Brown, E. T. and Huh, Y., 1996. Fluvial geochemistry of the eastern slope of the northeastern Andes and its foredeep in the drainage of the Orinoco in Colombia and Venezuela. Geochimica et Cosmochimica Acta, 60: 2949-2976.

Fairchild, I. J., Bradby, L., Sharp, M. and Tison, J.-L., 1994. Hydrochemistry of carbonate terrains in alpine glacial settings. Earth Surface Processes and Landforms, 19: 33-54.

Fontes, J.-C., Gasse, F. and Gilbert, E., 1996. Holocene environmental changes in Lake Bangong basin (Western Tibet). Part 1: Chronology and stable isotopes of carbonates of a Holocene lacustrine core. Palaeogeography, Palaeoclimatology, Palaeoecology, 120: 25-47.

Fort, M., 1996. Late Cenozoic environmental changes and uplift on the northern side of the central Himalaya: a reappraisal from field data. Palaeogeography Palaeoclimatology Palaeoecology, 120: 123-145.

France-Lanord, C., 1987. Chevauchement, métamorphisme et magmatisme en Himalaya du Népal central. Etude isotopique H, C, O. Ph.D. Thesis, INPL, Nancy, France.

France-Lanord, C. and Le Fort, P., 1988. Crustal melting and granite genesis during the Himalayan collision orogenesis. Transactions of the Royal Society of Edinburgh Earth Sciences, 79: 183-195.

France-Lanord, C. and Derry, L. A., 1997. Organic carbon burial forcing of the carbon cycle from Himalayan erosion. Nature, 390: 65-67.

France-Lanord, C., Derry, L. A., Le Fort, P., Mugnier, J.-L. and Gajurel, A. P., 1995. Silicate and carbonate weathering in the high Himalaya: Chemistry, C and Sr isotopic composition of the river system of Central Nepal., V. M. Goldschmidt Conference, 46.

Friedman, I. and O'Neil, J. R., 1977. Compilation of stable isotope fractionation factors of geochemical interest. In Data of Geochemistry, Vol. 440 - K.K. (ed. M. Fleischer), pp. 1-114. Geological Survey.

Gaillardet, J., Dupré, B. and Allègre, C. J., 1995. A global geochemical mass budget applied to the Congo Basin rivers: Erosion rates and continental crust composition. Geochimica et Cosmochimica Acta, 59, 3469-3485.

Gaillardet, J., Dupré, B., Allègre, C. J. and Négrel, P., 1997. Chemical and physical denudation in the Amazon river basin. Chemical Geology, 142: 141-173.

Galy, A., France-Lanord, C. and Derry, L. A., submitted. The Strontium isotopic budget of Himalayan rivers in Nepal and Bangladesh.

Gansser, A., 1964. Geology of the Himalayas. Intersciences Publishers, L.U.

Goddéris, Y. and François, L. M., 1996. Balancing the Cenozoic carbon and alkalinity cycles: Constraints from isotopic records. Geophysical Research Letters, 23: 3743-3746.
GRDC, 1994. Hydrological Regimes of the 20 largest rivers of the Wold - A compilation of the GRDC Database - No. 5. Global Runoff Data Centre.
Grout, H., 1995. Caractérisation physique, minéralogique, chimique et signification de la charge particulaire et colloïdale de rivières de la zone subtropicale. Ph.D. Thesis, Aix-Marseille, France.
Handa, B. K., 1969. Chemical composition of monsoon rains over Calcutta. Part I. Tellus, 22: 95-100.
Handa, R. K., 1972. Geochemistry of the Ganga River Water. Indian Geohydrology, 2: 71-78.
Harris, N., Bickle, M., Chapman, H., Fairchild, I., and Bunbury, J., 1998. The significance of Himalayan rivers for silicate weathering rates: evidence from the Bhote Kosi tributary. Chemical Geology, 144: 205-220.
Hasnain, S. I. and Thayyen, R. J., 1996. Sediment transport and solute variation in meltwaters of Dokriani glacier (Bamak), Garhwal Himalaya. Journal Geological Society of India, 47: 731-739.
Henning, D., 1989. Atlas of the surface heat balance of the continents. Gebrüder Borntraeger.
Hossain, M., Aminul Islam, A. T. M. and Kumar Saha, S., 1987. Floods in Bangladesh. Universities Research Centre.
Hurtrez, J.-E., 1998. Analyse géomorphologique des interactions Tectonique-Erosion dans le système Himalayen. Ph.D. Thesis, Montpellier, France.
Krishnamurthy, R. V. and Bhattacharya, S. K., 1991. Stable oxygen and hydrogen isotope ratios in shallow ground waters from India and a study of the role of evapotranspiration in the Indian monsoon. In H. P. Taylor, J. R. O'neil, & I. R. Kaplan (Eds.), Stable isotope Geochemistry : a tribute to Samuel Epstein (pp. 187-193). Geochemical Society.
Krishnaswami, S., Trivedi, J. R., Sarin, M. M., Ramesh, R. and Sharma, K. K., 1992. Strontium isotopes and rubidium in the Ganga-Brahmaputra river system: Weathering in the Himalaya, fluxes to the Bay of Bengal and contributions to the evolution of oceanic $^{87}Sr/^{86}Sr$. Earth and Planetary Science Letters: 109: 243-253.
Le Fort, P., 1989. The Himalayan orogenic segment. In A. M. C. Sengör (Eds.), Tectonic evolution of the Tethyan regions. Proceedings of the NATO ASI meeting, Istanbul, October 1985. Reidel Publ. Co.
Le Fort, P. and France-Lanord, C., 1995. Granites from Mustang and surrounding regions. Journal of Nepal Geological Society, 11: 53-57.
Ludwig, W., Amiotte-Suchet, P. and Probst, J.-L., 1996. River discharges of carbon to the world's oceans: determining local inputs of alkalinity and of dissolved and particulate organic carbon. Compte Rendu de l'Académie des Sciences, 323: 1007-1014.
Mc Cauley, S. E. and De Paolo, D. J, 1997. The marine $^{87}Sr/^{86}Sr$ and $\delta^{18}O$ records, Himalayan Alkalinity fluxes, and Cenozoic climate Models. in W.In W. F. Ruddiman (Eds.), Uplift and Climate Change (pp.). New York: Plenum Press.
Meybeck, M., 1987. Global chemical weathering of surficial rocks estimated from river dissolved loads. American Journal of Science, 287: 401-428.
Mook, W. G. and Tan, F. C., 1991. Stable Carbon Isotopes in Rivers and Estuaries. In E. T. Degens, S. Kempe, & J. E. Richey (Eds.), Biogeochemistry of Major World Rivers (pp. 245-264). John Wiley & Sons Ltd.
Mook, W. G., Bommerson, J. C. and Staverman, W. H., 1974. Carbon isotope fractionation between dissolved bicarbonate and gaseous carbon dioxide. Earth and Planetary Science Letters, 22: 169-176.
Moore, W. S., 1997. High fluxes of radium and barium from the mouth of the Ganges-Brahmaputra River diring low river discharge suggest a large groundwater source. Earth and Planetary Science Letters, 150: 141-150.
Négrel, P., Allègre, C. J., Dupré, B., and Léwin, E., 1993. Erosion sources determined by inversion of major and trace element ratios and strontium isotopic ratios in river water: the Congo basin case. Earth and Planetary Science Letters, 120: 59-76.
Palmer, M. R. and Edmond, J. M., 1992. Controls over the strontium isotope composition of river water. Geochimica et Cosmochimica Acta, 56: 2099-2111.
Pawellek, F. and Veizer, J., 1995. Carbon cycle in the upper Danube and its tributaries: $\delta^{13}C_{DIC}$ constraints. Israel Journal of Earth Sciences, 43: 187-194.
Pêcher, A., 1978. Déformation et métamorphisme associés à une zone de cisaillement. Exemple du grand chevauchement central himalayen (M.C.T.), transversale des Annapurnas et du Manaslu, Népal. Ph.D. Thesis, Joseph Fourier Univ., Grenoble, France.
Pegram, W. J., Krishnaswami, S., Ravizza, G. E. and Turekian, K. K., 1992. The record of sea water $^{187}Os/^{186}Os$ variation through the Cenozoic. Earth and Planetary Science Letters, 113: 569-576.
Quade, J., Roe, L., DeCelles, P. G. and Ojha, T. P., 1997. The late Neogene 87Sr/86Sr record of lowland Himalayan rivers. Science, 276: 1828-1831.
Rao, K. L., 1979. India's water wealth. Orient Longman limited.

Raymo, M. E. and Ruddiman, W. F., 1992. Tectonic forcing of late Cenozoic climate. Nature, 359: 117-122.

Richter, F. M., Rowley, D. B. and DePaolo, D. J., 1992. Sr isotope evolution of seawater: the role of tectonics. Earth and Planetary Science Letters, 109: 11-23.

Sarin, M. M. and Krishnaswami, S., 1984. Major ion chemistry of the Ganga-Brahmaputra river systems, India. Nature, 312: 538-541.

Sarin, M. M., Krishnaswami, S., Dilli, K., Somayajulu, B. L. K. and Moore, W. S., 1989. Major ion chemistry of the Ganga-Brahmaputra river system: Weathering processes and fluxes to the Bay of Bengal. Geochimica et Cosmochimica Acta, 53: 997-1009.

Sarin, M. M., Krishnaswami, S., Trivedi, J. R. and Sharma, K. K., 1992. Major ion chemistry of the Ganga source Waters : Weathering in the high altitude Himalaya. Earth and Planetary Science, 101: 89 - 98.

Seeber, L. and Gornitz, V., 1983. River profiles along the Himalayan arc as indicators of active tectonics. Tectonophysics, 92: 335-367.

Shieh, Y.N. and Taylor, H.P., 1969. Oxygen and carbon isotope studies of contact metamorphism of carbonate rocks. Journal of Petrology, 10: 307-331.

Sequeira, R. and Kelkar, D., 1978. Geochemical implications of summer monsoonal rainwater composition over India. Journal of Applied Meteorology, 17: 1390-1396.

Singh, S. K., Trivedi, J. R., Pande, K., Ramesh, R. and Krishnaswami, S., 1998. Chemical and Sr, O, C, isotopic compositions of carbonates from the Lesser Himalaya: Implications to the Sr isotope composition of the source waters of the Ganga, Ghaghara and the Indus Rivers. Geochimica et Cosmochimica Acta, 62: 743-755.

Solomon, D. K. and Cerling, T. E., 1987. The annual Carbon Dioxide Cycle in a Montane Soil: Observations, Modeling, and Implications for weathering. Water Resources Research, 23: 2257-2265.

Subramanian, V., Sitasawad, R., Abbas, N. and Jha, P. K., 1987. Environmental Geology of the Ganga River Basin. Journal Geological Society of India, 30: 335-355.

Tsunogai, S., Saito, O., Yamada, K. and Nakaya, S., 1972. Chemical composition of oceanic aerosol. Journal of Geophysical research, 77: 5283-5292.

Upreti, B. N. and Le Fort, P., in press.. Lesser Himalayan crystalline nappes of Nepal: problems of their origin. In A. Macfarlane, R. B. Sorkhabi, & J. Quade (Eds.), Himalaya and Tibet: mountain roots to mountain tops. GSA special paper N° 328.

Vennum, W. R., 1980. Evaporite encrustations and sulfide oxidation products from the southern Antartic Peninsula. New Zealand Journal of Geology and Geophysics, 23: 499-505.

Wake C. P., Mayewski, P. A. and Spencer, M. J., 1990. A review of central Asian glaciochemical data. Annals of Glaciology, 14: 301-306.

Wake, C. P., Mayewski, P. A., Zichu, X., Ping, W. and Zhongqin, L., 1993. Regional distribution of monsoon and desert dust signals recorded in Asian glaciers. Geophysical Research Letters, 30: 1411-1414.

Williams, M. W., Yang, D., Liu, F., Turk, J. and Melack, J. M., 1995. Controls on the major ion chemistry of the Urumqi River, Tian Shan, People's Republic of China. Journal of Hydrology, 172: 209-229.

Figure captions

Fig. 1 : Map of the Ganges and Brahmaputra basin and location of river samples and maps of figure 2. When several samples were taken at the same location only the first sample is labelled on the map. MFT: Main frontal thrust is the southernmost Himalayan thrust, thrusting the Siwaliks over the Gangetic plain. MCT : Main Central Thrust, thrusting the High Himalaya Crystalline over the Lesser Himalaya, is mostly located at the foot of the high range (Seeber and Gornitz, 1983).

Fig. 2 : Geological maps of Narayani watershed (a) and Karnali watershed (b) with water samples. When several samples have been taken at the same location only the first sample is labelled on the map. Geology after Colchen et al. (1986); Le Fort and France-Lanord (1995) and Upreti and Le Fort (in press). TSS = Tethian Sedimentary Series. HHC = High Himalaya Crystalline. LH = Lesser Himalaya. HHL = High Himalaya Leucogranite. LHN = Lesser Himalaya Nappe.

Fig. 3 : Triangular plots representing the relative abundance of major cation and anion charges. Ca is the dominant cation and Mg remains low in silicate drainage. SO_4^{2-} typically represents 10 to 20% of the anion charge. Cl^- is only significant in rivers draining the Mustang graben conglomerate.

Fig. 4 : River profile of the Kali Gandaki, from the source above Lo Mantang (Mustang) to the outflow of the Narayani in the Gangetic plain. a) Topographic profile of the river and average crest altitude (Hurtrez,1998). The breaks in the slope of the river profile underline the zones of intense physical erosion. Rocks of the Tethian sedimentary series (TSS) are separated from the High Himalayan Crystalline (HHC) by the Southern Tibetan Detachment System (STDS). The HHC are thrust over the Lesser Himalaya (LH) along the Main Central Thrust (MCT). b) average precipitation over the river basin from kriging of meteorological data of Nepal (Hurtrez,1998). c) Total Dissolved Solid (TDS). d) $\delta^{13}C_{DIC}$ decreases from north to south. In the north $\delta^{13}C_{DIC} \approx 0$ ‰, implying an inorganic origin of the carbon, while to the south, soil respiration becomes important. e) The ratio of sulfate to bicarbonate (X_{SO_4}) that largely reflects the contribution of the southern part of the TSS in this basin. f) silicate to carbonate weathering ratio (X_{Sil}) as defined in appendix.

Fig. 5 : Isotopic composition of dissolved inorganic carbon ($\delta^{13}C_{DIC}$) versus ratio of $[SO_4^{2-}]$ over $([SO_4^{2-}]+[HCO_3^-])$ termed (X_{SO_4}). Curves describe water characteristics for alteration driven by variable mixtures of sulphuric acid and carbonic acid of biologic

origin. Curves are drawn for different proportions of altered silicate to carbonate, assuming that both mineral are altered in the same amount by each acid. $\delta^{13}C$ of carbonate = 0‰, $\delta^{13}C$ of soil CO_2 = -18‰.

Fig. 6a : Plot of $\delta^{13}C_{DIC}$ versus X_{SO_4} in the Kali Gandaki head waters. Data for thermal springs sampled near the river show high $\delta^{13}C$ values, implying a metamorphic origin for the CO_2. The mixing curve corresponds to the alteration by sulphuric acid and respired carbonic acid of 70% of carbonate and 30% of silicate. The fact that rivers plot to the right of the mixing curve implies that CO_2 rich in ^{13}C is involved in the alteration reaction in addition to biologic CO_2. The contribution of metamorphic CO_2 dissolved in ground water as sampled in thermal springs is clearly identified at several locations.

Fig. 6b : Plot of $\delta^{13}C_{DIC}$ versus X_{SO_4} for main Himalayan rivers, Ganges and Brahmaputra. The mixing trend corresponds to the alteration by sulphuric acid and biologic carbonic acid of 70% of carbonate and 30% of silicate. Most samples are compatible with a model of alteration driven by soil CO_2 mixed with variable proportion of H_2SO_4. The 3 labelled samples are close to the MCT, where spring waters are known and may locally influence the TDS.

Fig. 7 : Seasonal variation of the water discharge and chemistry of the Trisuli river at Betrawati for TDS, X_{SO_4}, X_{Sil} and $\delta^{13}C_{DIC}$. The shaded area corresponds to the monsoon season. Water discharge data are from the Dept. of Hydrology and Meteorology of Nepal.

Fig. 8 : Seasonal variation of TDS versus X_{SO_4} for the Trisuli river at Betrawati. The lowest TDS values occur at the beginning and end of the monsoon. The lowest X_{SO_4} values are found during the peak monsoon, while the highest X_{SO_4} occur during the dry season.

Fig. 9 : K* versus Mg* concentration relationship for Himalayan rivers. Concentrations have been corrected for cyclic contribution according to § 5.1. Open symbols: rivers draining carbonate and silicate formations; Grey symbols: rivers draining only silicate formations. The line represents [Mg]*/[K]* ratios of 1. Some samples with extreme concentrations have been excluded. The data show that silicate weathering contributes a small fraction of the dissolved Mg budget in most rivers.

Appendix : Definition of the X_{sil}

Assuming negligible anthropogenic contributions for major rivers, and correcting for cyclic contribution (cf. § 5.1), equation (1) can be simplified in the equation (2) :

$$[X]_{river} = X_{cyclic}+X_{evaporite}+X_{carbonate}+X_{silicate}+X_{sulfide}+X_{anthropogenic} \quad (1)$$

$$[X]^*_{river}=X_{evaporite}+X_{carbonate}+X_{silicate}+X_{sulfide} \quad (2)$$

Our modelling is based on four straightforward simplifications of the budget equations. First, chloride is only derived from evaporites and from precipitation. Second, the dissolution of carbonate does not contribute to the dissolved sodium and potassium. Third, evaporite weathering yields only NaCl. Finally, sulfate is entirely derived from sulfide oxidation. With these assumptions, we can simplify the equation (1) as follows :

$$[Cl]^* = Cl_{evaporite} \quad (3)$$

$$[Na]^* = Cl_{evaporite} + Na_{silicate} \quad (4)$$

$$[SO_4]^* = SO_{4sulfide} \quad (5)$$

$$[K]^* = K_{silicate} \quad (6)$$

$$[Ca]^* = Ca_{carbonate} + Ca_{silicate} \quad (7)$$

$$[Mg]^* = Mg_{carbonate} + Mg_{silicate} \quad (8)$$

Equations (7) and (8) are difficult to solve because of the uncertainty about silicate versus carbonate contributions. In most river system, Sr isotopic composition is a useful additional constraint, but in the case of Himalayan rivers the Sr isotopic budget is complex and cannot be used for this purpose (Palmer and Edmond, 1992; Krishnaswami et al., 1992; Blum et al., 1998; Harris et al., 1998; Singh et al., 1998). Chemical composition of the eroded rocks is therefore utilized as the substitute criterion. The Himalayan crust is dominated by quartz, K and Na feldspars, and micas. Calcic silicates are not a major source of eroded material, except in the Formation II of the HHC (Colchen et al. 1986). A maximum estimate for the Ca/Na ratio of silicates is given by the mean whole-rock composition of the eroded formations. These are 0.25 for the HHC (France-Lanord and Derry, 1997), 0.30 for the LH (Pêcher, 1978) and 0.06 for leucogranitic rocks (France-Lanord and Le Fort, 1988). A minimum ratio is given by the analyses of plagioclase in the HHC of central Nepal, with an average Ca/Na ratio of 0.18 (Brouand, 1989). On this basis we consider that the Ca/Na ratio delivered to the dissolved load must be close to 0.2 which allows us to rewrite equation (7) where all species are in μmol/l:

$$[Ca]^* = Ca_{carbonate} + Na_{silicate} \times 0.2 \quad (9)$$

The budget of Mg is more difficult to assess. Dolomite is present in all bed load samples, except in the Upper Kali Gandaki basin, and therefore an unknown proportion

of Mg is derived from carbonate. Marked positive relationship between [Ca] and [Mg] suggest that a large proportion of the Mg is derived from dolomite weathering. On the silicate side, the main reaction which can release Mg in Himalaya is the weathering of biotite and, to a lesser extent, chlorite and garnet. These reactions are incongruent and Mg is retained in weathering by products such as hydrobiotite, vermiculite or smectite, all common in the Himalayan soils (Bäumler and Zech, 1994; Grout, 1995). The $Mg_{silicate}$ contribution can be estimated using the [Mg]* versus [K]* relationship (Fig 9). In this diagram, rivers draining both carbonate and silicate formations have [Mg]*/[K]* ratios above 1, and [Mg]* appears to be independent of [K]*. In contrast, a marked correlation for catchments draining basins of pure silicate lithology, most having low [Mg]*/[K]* ratios between 1 and 0.2. Similar ratios have been obtained on Western Himalayan streams draining gneissic basins (Blum et al, 1998). Dissolved Mg/K vary during silicate weathering because (1) K can be released by weathering of feldspars and muscovite which do not release Mg and (2) Mg and K are fractionated during secondary mineral formation in different directions depending on micas alteration reactions and alteration conditions (e.g. Mc Bride, 1994). Therefore we will examine silicate weathering budget with $Mg/K = 0.5 \pm 0.25$ which corresponds to most of the measured ratios in silicate catchments. Equation 8 can then be expressed as:

$$[Mg]^* = Mg_{carbonate} + K_{silicate} \times 0.5 \pm 0.25 \ (\text{in } \mu\text{mol/l}) \qquad (10)$$

While there is a large uncertainty to this ratio, it does not strongly affect the budget of silicate to carbonate weathering. This budget can now be calculated for main rivers because $K_{silicate}$ is always low compared to $Ca_{carbonate}$ and $Mg_{carbonate}$.

The silicate to carbonate budget can then be expressed by the ratio of dissolved cations from silicates over the sum of dissolved cations from silicates plus carbonates. This can be expressed as ratio of equivalent cationic charge by combining equations 3, 4, 6, 9 and 10 :

$$X_{sil} = (1.4 \times (Na^* - Cl^*) + 2 \times K^*)/(Na^* + K^* + 2 \times Mg^* + 2 \times Ca^*)$$

Table 1 - Chemical data from the Kali Gandaki and tributaries

Sample	River	Location	Date	Altitude m	Temp °C	pH	TDS mg/l	$\delta^{13}C$ ‰	HCO_3	F^-	Cl^-	SO_4^{2-}	NO_3^-	Na^+	K^+	Mg^{2+}	Ca^{2+}	Si
									μmol/l									
LO 25	Nangyal	Lo Mantang	May.20.93	3695			161	-6.7	1779	29	11	89	0.3	77	21	109	839	148
LO 49	Kali	Lo Mantang	May.20.93	3550	5		316	+1.3	2936	36	929	111	bdl	1254	106	184	1186	250
NH 133	Kali	Lo Mantang	Apr.30.95	3575	9.6	7.8	218	-3.2	2273	13	270	97	bdl	455	53	138	982	189
LO 63	Tsarang	Lo Gekar	May.21.93	3920	4.5		212	-0.3	1909	17	17	402	bdl	115	25	218	1082	127
LO 23	Tsarang	Tsarang	May.19.93	3400			394	+1.4	4127	31	38	371	bdl	697	48	327	1759	270
LO 15	Ghemi	Ghemi	May.19.93	3385	6.3		214	-4.3	2108	14	34	300	0.3	134	47	247	1035	91
LO 96	Narsing	Chhuksang	May.24.93	2900	10		880	+3.9	3594	53	1740	3687	15	4202	390	2246	1825	68
LO 1	Kali	Kagbeni	May.16.93	2800	14		358		2330	22	770	962	bdl	937	79	761	1244	78
NAG 21	Kali	Kagbeni	Nov.25.95	2790	3.8	8.5	426	+0.4	2932	13	787	1096	14	912	82	835	1628	93
NH 147	Kali	Jomsom	May.3.95	2675	8.4	8.4	400	+0.3	2600	11	880	1081	bdl	1027	105	878	1378	83
LO 99	Thini	Thinigaon	May.26.93	2650			293	-2.1	2527	8.4	19	722	12	170	31	954	946	40
LO 103	Marpha	Marpha	May.26.93	2635			183	-5.0	1543	2.6	13	458	bdl	20	16	432	784	27
LO 101	Kali	Marpha	May.26.93	2530	10		348	-1.4	2259	19	622	1019	bdl	778	76	825	1208	nd
NAG 30	Kali	Chairogaon	Dec.1.95	2626	6.3	9.3	418	+0.3	2761	12	640	1221	12	826	75	935	1539	92
NAG 32	Kali	Khobang	Dec.2.95	2530	2.0	8.8	416	+0.1	2811	12	663	1171	12	833	74	966	1490	92
NAG 34	Kali	Koketani	Dec.2.95	2500	11	9.4	382	-1.0	2646	8.9	465	1102	5.3	573	77	943	1389	78
NAG 39	Kali	Dana	Dec.3.95	1450	9	8.5	361	-1.3	2624	12	528	906	12	600	87	771	1371	99
NAG 41	Miristi	Banskot	Dec.4.95	1490	8.9	8.5	165	-3.3	1653	2.6	47	210	2.3	85	43	246	752	85
NH 10	Kali	Tatopani	Mar.15.95	1180	9.4	8.6	362	-2.2	2375§	10	677	826	bdl	759	80	774	1309	109
NAG 43	Kali	Tatopani	Dec.5.95	1180	8.7		314	-3.0	2455	8.4	361	734	bdl	423	72	679	1214	92
NH 31	Mayongd	Tatopani	Mar.14.95	905	11	8.3	256	-7.1	2251§	6.3	84	387	bdl	485	65	491	904	94
NH 8	Kali	Beni	Mar.13.95	815	12	8.6	290	-9.5	2220§	8.9	394	570	bdl	495	54	622	1072	103
NAG 45	Kali	Baglung	Dec.6.95	740	13	8.6	231	-4.8	2004	6.8	188	433	6.8	254	70	451	921	101
NH 7	Andhi	Waling	Mar.12.95	705	22	8.8	269	-10.1	3221§	5.3	44	57	bdl	69	28	811	872	100
LO 310	Kali	Ramdi	Jun.10.93	460	22		186	-8.9	1911	9.5	73	212	0.3	113	50	362	762	75
NH 6	Kali	Ramdi	Mar.12.95	460	17	8.8	264	-6.5	2389§	7.9	202	351	bdl	269	62	636	948	108
NAG 5	Kali	Ramdi	Nov.13.95	460	18	8.4	206	-9.0	2095	6.3	93	262	bdl	135	49	493	774	59
LO 306	Kali	Kot	Jun.9.93	305	26		162	-7.8	1651	12	56	191	3.7	101	50	338	635	78

§ : alkalinity field titration. bdl: below the detection limit. nd: not determined

Table 2 - Chemical data from the Trisuli river and tributaries

Sample	River	Area	Date	Altitude	Temp ℃	pH	TDS mg/l	$\delta^{13}C$ ‰	HCO_3^-	F^-	Cl^-	SO_4^{2-}	NO_3^-	Na^+	K^+	Mg^{2+}	Ca^{2+}	Si
									μmol/l									
LO 237	Lari	Lari valley	Jun.5.93	4245			40	-9.4	428	2.6	4	37	12	5	14	102	149	17
LO 238	Mailung	Paigutang	Jun.5.93	4020			18	-8.6	155	1.5	3	22	22	17	16	32	60	19
LO 257	Langtang	Syabru Bensi	Jun.6.93	1480			33	-2.9	297	10	7	45	0.3	51	25	19	141	50
NH 100	Langtang	Syabru Bensi	Apr.14.95	1455	11	7.8	50	-4.8	432	13	14	82	bdl	110	21	42	205	114
NH 102	Bhote Kosi	Syabru Bensi	Apr.14.95	1440	12	7.9	128	-2.5	1174	8.9	58	203	bdl	175	32	209	514	113
LO 256	Trisuli	Syabru Bensi	Jun.6.93	1430	13		79	-2.0	784	11	23	87	13	80	29	88	355	60
LO 258	Trisuli	Betrawati	Jun.6.93	750	18		73	-4.9	739	11	18	75	6.0	84	28	76	327	64
TRI 19/6	Trisuli	Betrawati	Jun.19.93	750			63	-7.2	644	6.8	16	56	8.2	56	24	56	296	51
TRI 6/7	Trisuli	Betrawati	Jul.6.93	750			71	-10.4	760	6.3	17	42	bdl	57	51	51	328	80
TRI 15/7	Trisuli	Betrawati	Jul.15.93	750			81	-8.6	897	6.8	14	41	bdl	44	39	49	409	57
TRI 1/8	Trisuli	Betrawati	Aug.1.93	750			73	-10.0	784	5.8	15	42	bdl	54	51	51	341	82
TRI 15/8	Trisuli	Betrawati	Aug.15.93	750			70	-9.7	737	5.3	19	46	bdl	67	39	49	324	75
TRI 1/9	Trisuli	Betrawati	Sep.1.93	750			68	-9.0	694	5.3	43	54	bdl	93	48	77	278	73
TRI 15/9	Trisuli	Betrawati	Sep.15.93	750			60	-9.2	610	5.3	17	55	bdl	71	29	65	255	94
TRI 1/10	Trisuli	Betrawati	Oct.1.93	750			64	-10.4	642	5.8	26	57	2.3	94	35	73	257	107
TRI 15/10	Trisuli	Betrawati	Oct.15.93	750			79	-5.4	766	8.4	35	85	6.3	124	33	94	319	114
TRI 1/11	Trisuli	Betrawati	Nov.1.93	750			80	-6.7	779	7.9	33	84	bdl	129	37	93	318	116
TRI 1/12	Trisuli	Betrawati	Dec.1.93	750			95	-8.1	911	9.5	49	111	1.5	170	38	117	376	127
TRI 4/4	Trisuli	Betrawati	Apr.4.94	750			107		1027	9.5	49	133	1.9	200	43	136	418	125
KN 76	Tadi	Source	Mar.21.94	3665			11		80	1.6	4.1	21	17	26	9	8	46	68
KN 82	Hundi	Shisipur	Mar.21.94	2130			12		83	2.3	4.5	21	19	50	8	10	35	103
KN 84	Tadi	Ghyangphedi	Mar.21.94	2050			32		321	4.4	5.9	32	13	54	17	16	153	110
KN 93	Tadi	Satbise	Mar.23.94	945			27		262	3.9	6.7	32	10	99	20	20	94	178
KN 95	Chake	Samundratar	Mar.23.94	935			30		331	3.7	11	16	0.2	175	26	22	67	263
KN102	Likhu	Bhadrutar	Mar.24.94	750			55		598	7.3	23	30	0.2	230	45	47	159	310
LO 316	Trisuli	Adamghat	Jun.10.93	465	21		84	-8.4	889	8.9	19	62	0.3	94	32	84	370	93
LO 304	Trisuli	Gumaune	Jun.9.93	320	21		115	-5.7	1121	11	63	140	0.3	119	35	152	505	84

Table 3 - Chemical data for other rivers of the Narayani basin and Bothe Kosi at Kodari.

Sample	River	Location	Date	Altitude m	Temp °C	pH	TDS mg/l	$\delta^{13}C$ ‰	HCO_3^-	F^-	Cl^-	SO_4^{2-}	NO_3^-	Na^+	K^+	Mg^{2+}	Ca^{2+}	Si
									μmol/l									
BHURI GANDAKI																		
MO 107	Mati	Arughat	May.12.97		27		78	-11.6	887		19	28	1.1	255	59	76	248	
MO 125	Sueli		May.14.97		30		49	-12.7	580		21	4	bdl	194	23	58	138	
LO 300	Bhuri Gandaki	Benighgat	Jun.9.93	410	18		122	-3.9	1187	8.4	24	174	13	75	29	176	559	59
MARSYANDI																		
NAG 24	Marsyandi	source	Nov.28.95	5050	0		606	-1.3	2937	2.1	4.1	2852	bdl	48	23	1353	2925	30
HF 131	Miyardi		May.7.93	3920			18		206	0.6	3.7	5	bdl	7	12	7	93	12
MO 58	Chepe		May.7.97	3100			17	-8.4	168		1.6	17	8.6	30	15	6	77	
MO 79	Khota		May.9.97	1700	15		42	-10.9	449		3.3	31	bdl	69	68	34	154	
MO 28	Dordi	Darimbote	May.4.97	1450	10		48	-5.9	414		5.1	101	5.7	53	37	29	239	
MO 100	Marsel		May.11.97	590	23		55	-11.3	633		17	17	bdl	235	49	60	140	
LO 314	Marsyandi	Markichok	Jun.10.93	435	20		127	-6.0	1173	11	140	170	0.3	157	45	165	561	80
SETI KHOLA																		
HF 126	Chhar	Rambong	May.5.93	3785			6.4		73	0.5	3.2	1	bdl	5	8	7	26	2
HF 111	Chhar	Rambong	May.4.93	3680			8.3		72	0.5	3.3	5	bdl	18	11	8	20	48
HF 103	Madi	Siklis	May.2.93	1435			103	-7.5	1058	10	41	87	31	60	31	30	580	
HF 141	Madi	Khilang	May.10.93	1040			102		1086	3.7	45	77	1.3	81	43	40	542	31
NH 40	Sardi	Khadarjung	Mar.16.95	1185	17	8.5	133	-8.3	1341	4.7	10	153	bdl	58	82	205	555	169
NH 39	Seti	Khadarjung	Mar.16.95	1180	9.9	7.9	208	-3.4	1730§	7.4	190	430	bdl	228	54	329	918	83
NAG 3	Bijapur	Kundahar	Nov.11.95	870	21	8.1	149	-10.3	1670	3.7	68	64	3.7	87	51	290	578	136
LO 312	Seti	Kotre Bazar	Jun.10.93	585	26		179	-6.7	1893	9.5	42	171	0.3	87	57	332	738	107
LO 302	Seti	Sarang Ghat	Jun.9.93	325	26		162	-7.4	1688	8.4	33	174	0.3	102	51	322	636	120
NARAYANI																		
LO 308	Narayani	Nayaran Ghat	Jun.9.93	225	26		145	-8.0	1458	10	60	169	0.3	114	51	244	602	96
NH 1	Narayani	Nayaran Ghat	Mar.10.95	225	20	8.5	202	-5.6	2038§	10	148	245	bdl	230	50	439	739	143
NAG 49	Narayani	Nayaran Ghat	Dec.11.95	225	19	8.4	207	-7.1	2143	6.3	88	214	bdl	185	68	429	777	159
NH 20	Bothe Kosi	Kodari	Mar.17.95		6.5	8.2	107	-2.0	1169§	8.4	20	120	bdl	163	14	112	468	124

§ : alkalinity by field titration.

Table 4 - Chemical data for river from Karnali basin and Siwaliks.

Sample	River	Location	Date	Altitude	Tem °C	pH	TDS mg/l	$\delta^{13}C$ ‰	HCO_3^-	F^-	Cl^-	SO_4^{2-}	NO_3^-	Na^+	K^+	Mg^{2+}	Ca^{2+}	Si
									μmol/l									
NH 80	Thuli	Dunai	Mar.21.9	2030	8.3	8.5	234	-4.0	2089§	3.7	16	526	bdl	88	29	553	956	67
NAG 47	Thuli	Dunai	Nov.25.9	2030			229	-8.3	1852	2.6	222	512	17	147	64	498	954	57
NH 71	Tilla Nadi	Tatopani	Mar.21.9	2130	14	8.8	125	-10.5	1495§	7.7	31	77	bdl	58	82	205	555	
NAG 14	Bheri	Sampujighat	Nov.18.9	370	17	8.3	195	-7.9	2111	3.7	19	183	7.3	90	40	442	746	95
NAG	Bheri	Sampujighat	Jun.95	370			198		2176	2.4	32	156	bdl	84	70	354	830	84
NAG*	Bheri	Sampujighat	Aug.95	370			174		1985	1.8	18	96	0.6	40	53	304	748	87
NAG*	Bheri	Sampujighat	Sep.95	370			174		1920	2.6	14	149	bdl	56	38	393	678	106
94-16*	Bheri	Ghatgaun	Mar.27.9				222		2422	3.7	31	203	0.3	160	52	499	826	101
94-15	Karnali	Ghatgaun	Mar.25.9				161		1694	13	47	149	0.3	151	49	283	644	108
NAG 11	Karnali	Kotillaghat	Nov.17.9	100	20	8.6	229	-8.0	1595	7.9	29	131	6.6	198	46	432	896	146
NAG 19	Rapti	Darbang	Nov.21.9	290	19	8.6	229	-10.5	2590	7.4	26	141	bdl	144	62	456	893	155
NAG 10	Rapti	Bhabaniyapur	Nov.16.9	140	22	8.6	274	-9.3	3156	5.8	27	131	bdl	149	79	475	1136	151
94-05	Sarda	Luham	Mar.8.94	1400			200		2375	4.2	80	40	0.3	133	18	425	768	124
NAG 15	Sarda	Luham	Nov.16.9	1400			140	-10.1	1571	3.7	52	61	bdl	130	28	212	584	148
SIWALIKS																		
94-01	Chor	Upper part	Mar.2.94				670		7139	16	71	628	bdl	3488	124	1059	1373	175
94-02	Suraî	Upper part	Mar.4.94				599		6574	22	70	415	0.3	3729	108	1020	807	268
NH 3	Suraï	Tatopani	Mar.11.9		18	8.5	631	-8.6	6764§	14	46	217	bdl	3277	286	1148	974	320
94-03	Rangsing	Charange	Mar.5.94				331		3920	6.8	34	104	0.3	473	53	556	1264	132
94-13	Gadel	Palaite	Mar.23.9				325		3988	5.8	52	6	0.3	197	46	581	1326	199
94-14	Basunti	Bashanti	Mar.24.9				270		3292	6.8	33	14	3.5	138	43	360	1231	113
94-17	Kachali		Mar.29.9				403		4699	8.4	22	148	1.8	1768	84	794	789	203
94-18	Banka		Mar.29.9				477		5515	6.3	31	204	0.3	2167	95	833	1010	165

§ : alkalinity by field titration; * : sample filtred in the laboratory and non acidified.

Table 5 - Chemical data for rivers in Bangladesh

Sample	River	Location	Date	Temp ℃	pH	TDS mg/l	$\delta^{13}C$ ‰	HCO_3^-	F^-	Cl^-	SO_4^{2-}	NO_3^-	Na^+	K^+	Mg^{2+}	Ca^{2+}	Si
												μmol/l					
BGP 12	Tista	Kaunia	Aug.4.96	28	7.2	41	-11.9	350§	7.1	21	42	bdl	51	37	45	153	129
BGP 72	Tista	Kaunia	Mar.7.97	24	8.1	79	-8.6	817	13	34	78	bdl	221	41	121	258	nd
BGP 4	Ganges	Rajshahi	Aug.2.96	31	7.6	125	-10.1	1421§	10	94	76	0.3	175	69	201	466	127
BGP 65	Ganges	Rajshahi	Mar.3.97	24	8.5	374	-8.2	4412	10	234	64	2.7	619	110	612	1418	nd
BGP 15	Brahmaputra	Chilmari	Aug.5.96	29	7.6	105	-10.1	1114§	4.3	25	55	bdl	104	52	168	393	155
BGP 79	Brahmaputra	Chilmari	Mar.7.97	23	8.5	145	-8.3	1513	8.2	53	149	1.6	196	75	214	590	nd
BGP 51	Brahmaputra	Aricha Ghat	Feb.25.97	22	8.4	154	-9.2	1619	8.7	58	154	1.6	281	26	233	613	nd
BGP 39	Upper Meghna	Bhairab Bazar	Aug.13.96	30	7.2	38	-11.8	395§	3.5	30	21	2.5	84	18	68	108	129
BGP 0	Upper Meghna	Nangalband	Oct.20.94			47		512	2.6	25	7	1.6	113	37	86	117	126
BGP 20	Lower Meghna	Bhola	Aug.10.96	30	8.1	127	-9.0	1350§	7.6	78	77	23	229	41	182	489	129

§ : alkalinity by field titration.

Table 6 - Average chemical composition of river water in the G-B system

Zone	Catchment Type	n	$\delta^{13}C$ ‰	pH	TDS mg/l	HCO_3^-	Cl^-	SO_4^{2-}	Na^+	K^+	Mg^{2+}	Ca^{2+}	H_2SiO_4
						μmol/l							
North Flank	Composite	6	-3.1	8.5	270	2060	20	790	90	30	550	1220	80
Mustang	Graben	11	+0.2	8.7	410	2900	710	1080	1140	110	820	1420	130
South Flank	Composite	25	-8.4	8.3	160	1680	50	120	120	40	250	520	100
South Flank	Gneiss	11	-8.9	7.5	30	310	10	30	70	20	20	120	120
Ganges			-10.1	7.6	130	1420	90	80	180	70	200	470	130
Brahmaputra			-10.1	7.6	110	1110	20	60	100	50	170	390	160

All data are rounded average and therefore may not satisfy the charge neutrality.

Table 7 - Chemical composition of rain water in the Ganges-Brahmaputra basin

Source	Location	Area	Date	Type	n	TDS	HCO_3^-	F^-	Cl^-	SO_4^{2-}	NO_3^-	Na^+	K^+	Mg^{2+}	Ca^{2+}	Si
						mg/l					μmol/l					
(1)	Tibet	Everest	Spring 1986	snow	120				6.1	2.9	4.5	7.5			16	0.5
(1)	Nepal	Yala	1970-81	snow	55				9.9	2.4	2.1	11				
(2)	Nepal	Ngozumpa	1989-90	snow	30				0.3	0.1	0.1	0.3			0.2	
(2)	Tibet	Xixabangma	1990-91	snow	31				0.5	0.2	0.6	0.4			0.6	
(2)	Tibet	Qiang Yong	1990-91	snow	17				0.5	0.2	0.6	0.4			0.6	
(3)	Nepal	Likhu	1991-93	rain	73					9.4	4.2	13	4.9	17	29	
(4)	Nepal	Kathmandu	1995-96	rain	11	9.3	91	1.3	8.7	6.2	5.3	15	7.9	3.0	44	4.2
	Himalaya	Weighted Average					68§		7.4	4.7	3.9	10	2.2	6.1	22	0.8
(5)	India	Calcutta	1967	rain	112				41	35	4.6	41	8.4	15	48	62
(6)	India	Calcutta	1975	rain	56				28	7.8		37	4.4	4.9	17	
(6)	India	Delhi	1975	rain	56				18	4.4		30	5.9	3.7	29	
(6)	India	Gulmarg	1975	rain	28				8.7	3.5		20	3.1	6.6	22	
(4)	Bangladesh		monsoon 1996	rain	7	5.8	26	1.2	20	12	8.6	17	16	2.4	20	3.0
	Plain	Weighted Average					55§		29	19	4.8	35	6.6	9.0	34	

The very high concentration of Cl in Collins and Jenkins (1996) were excluded because the charge balance of these analyses imply no HCO_3^- in the rain and a deficit of cations. § : by charge balance. Sources : (1) : Wake et al. (1990); (2) : Wake et al. (1993); (3) : Collins and Jenkins (1996); (4) : this study ; (5) : Handa (1969); (6) : Sequeira and Kelkar (1978).

Table 8 : Chemical denudation rate for main sampled rivers

River	Location	Season	Discharge 10^9 m^3/yr	Surface 10^3 km^2	Silicate mm/yr	Carbonate mm/yr
Trisuli	Betrawati	Monsoon	4.2	4.6	0.007±3	0.033±15
Trisuli	Betrawati	Other	1.5	4.6	0.003±1	0.009±3
Trisuli	Betrawati	Year¶	5.8	4.6	0.005	0.021
Bheri	Sampujighat	Monsoon	10.3	12.3	0.011±2	0.131±29
Bheri	Sampujighat	Other	3.4	12.3	0.002±1	0.024±16
Bheri	Sampujighat	Year¶	13.7	12.3	0.005	0.060
Narayani	Narayangha	Year¶	49.4	31.8	0.007	0.052
Tista	Kaunia	Year¶	26.0	12.5	0.008	0.013
Brahmaputra	Chilmari	Year¶	612	583	0.004	0.021
Brahmaputra	GEMS	Year	612	583	0.005	0.018
Ganges	Rajshahi	Year¶	459	1060	0.002	0.013
Ganges	GEMS	Year	459	1060	0.003	0.011

¶ : Annual chemical denudation rates correspond to monsoonal rate over 4 months and dry season rates are the ramaining months. In order to calculate the chemical denudation rate an average density of 2.7 and 2.4 for silicate and carbonate were applied. GEMS : average data from UNEP GEMS/WATER Program.

Table 9 - Fluxes of dissolved element in the different zones of the Ganges and Brahmaputra basin

Rivers	Discharge	Surface	Cl^-	Na^+	K^+	Mg^{2+}	Ca^{2+}	HCO_3^-	SO_4^{2-}	H_2SiO_4
	10^9 m^3/yr	10^3 km^2				10^9 mol/yr				
Ganges	459	1060	40	128	29	93	252	713	39	59
Indian Shield¶	100	328	*26.8*	*82.4*	*5.2*	*37.1*	*69.3*	*256*	*5.4*	*17.8*
Himalaya§	206	176	*9.5*	*27.5*	*12.2*	*68.6*	*138*	*387*	*31.2*	*25.7*
Plain#	153	556	*3.8*	*18*	*12*	*-13*	*44.3*	*70.5*	*2.3*	*15.4*
±			114%	74%	10%	60%	34%	74%	83%	23%
Plain/Ganges	33%		10 ±11 %	14 ±10 %	41 ±4 %	-14 ±9 %	18 ±6 %	10 ±7 %	6 ±5 %	26 ±6 %
Brahmaputra	612	583	19	55	29	94	211	473	91	78
G-B	1071	1643	59	183	59	187	462	1185	130	137
World rivers	37400	148170	6120	8460	1240	5230	12500	31900	2060	6480

¶ : The Indian Shield contribution is the sum of each documented southern tributaries of the Ganges.
§ : The Himalaya are the sum of each main river that cross the MFT.
# : The plain contributions are the missing fluxes between the mouth and Himalayan + Indian Shield contribution. Relative uncertainties are the propagation of 5% and 15% uncertainties on the Himalayan and Indian Shield riverine concentration respectively. Therefore only K, Ca, Si and at a lesser extent alkalinity are significative.

Fig. 1

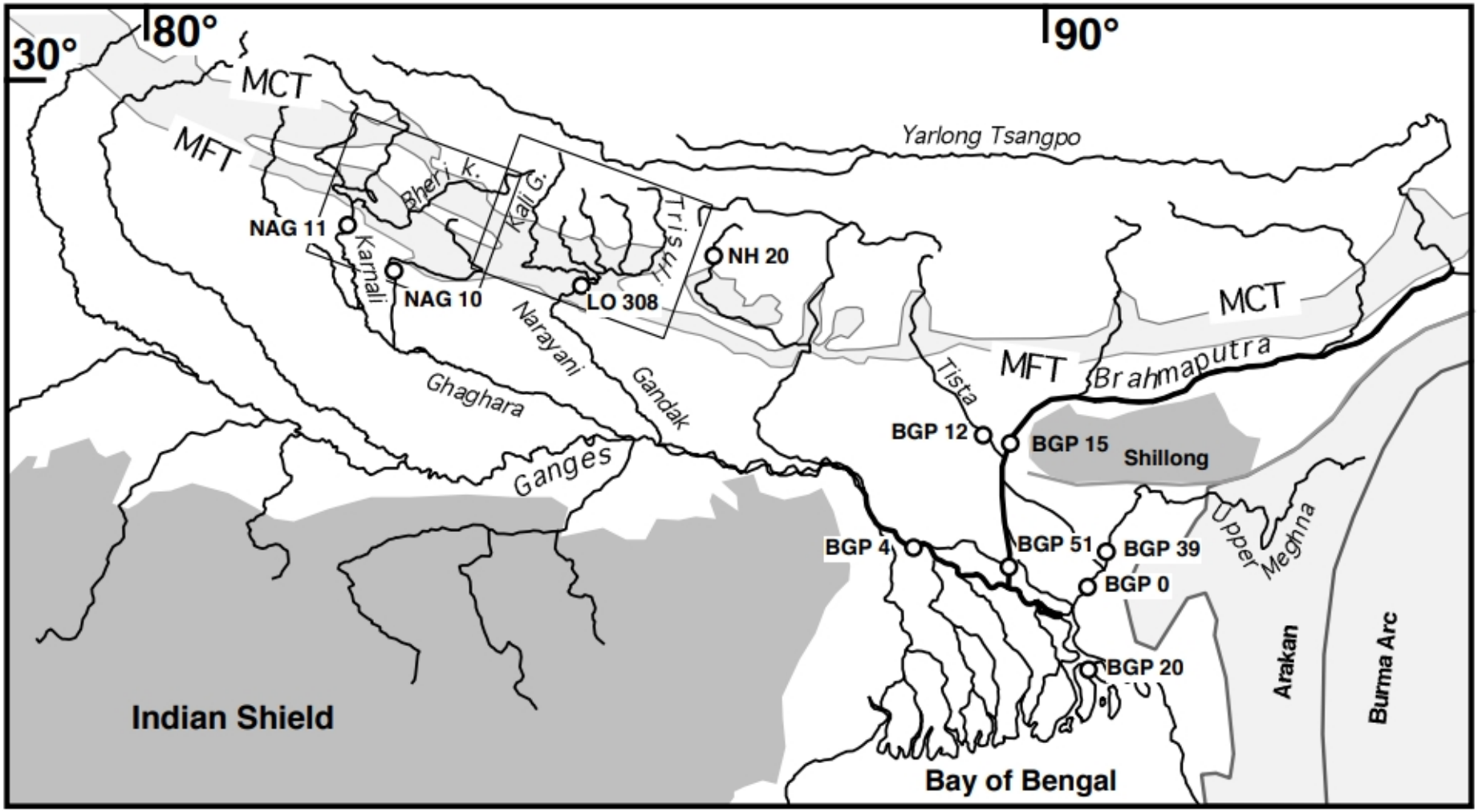
30°
80°
90°
MCT
MFT
Yarlong Tsangpo
Bheri k.
Kali G.
Trisuli
NAG 11
Karnali
NAG 10
LO 308
NH 20
Narayani
Gandak
Ghaghara
Ganges
MCT
MFT
Tista
Brahmaputra
BGP 12
BGP 15
Shillong
BGP 4
BGP 51
BGP 39
BGP 0
BGP 20
Upper Meghna
Arakan
Burma Arc
Indian Shield
Bay of Bengal

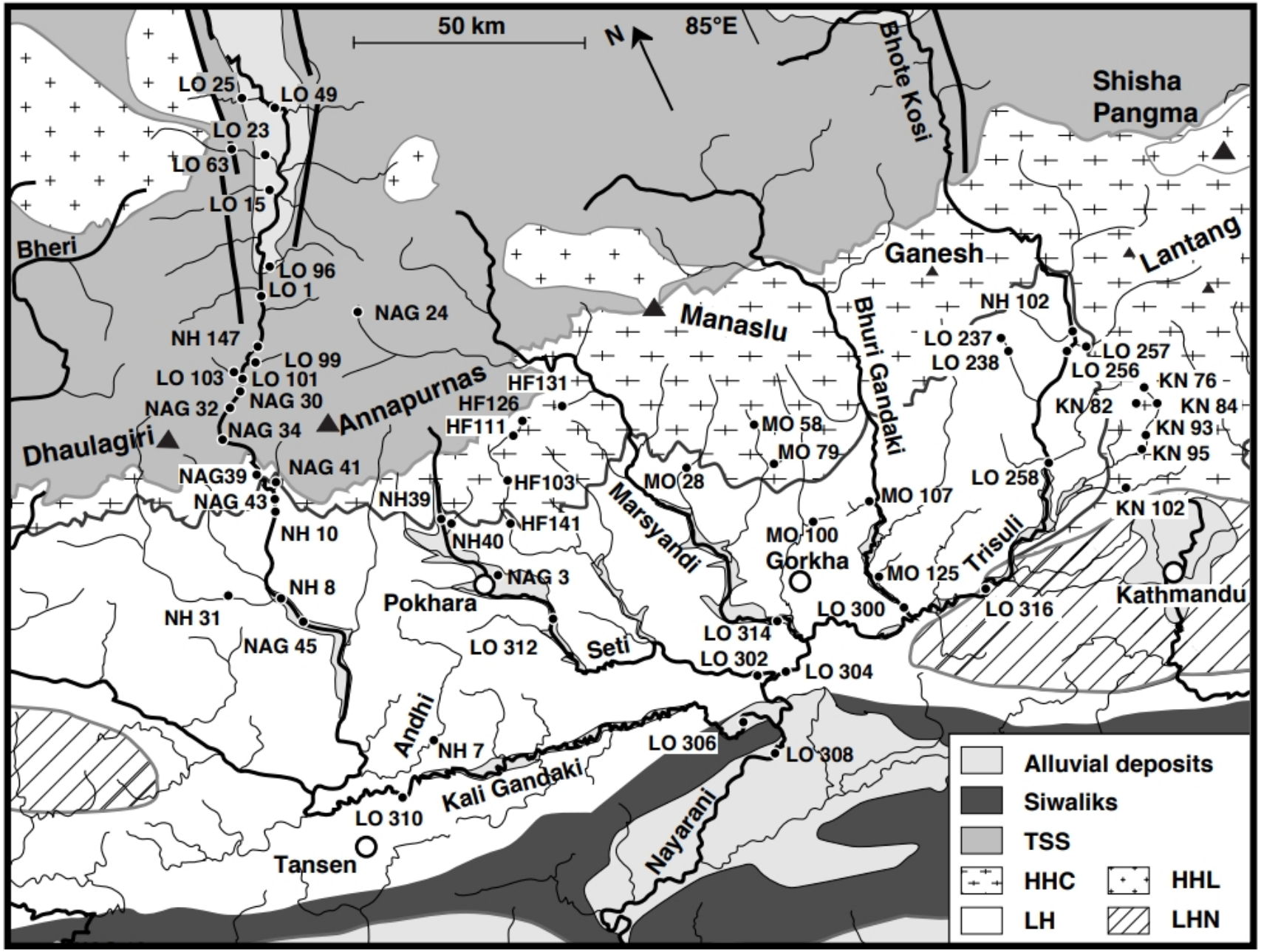
50 km
N
85°E
Bhote Kosi
Shisha Pangma
LO 25
LO 49
LO 23
LO 63
LO 15
Bheri
LO 96
LO 1
NAG 24
NH 147
LO 99
LO 103
LO 101
NAG 32
NAG 30
NAG 34
Dhaulagiri
Annapurnas
Manaslu
Ganesh
Lantang
Bhuri Gandaki
NH 102
LO 237
LO 238
LO 257
LO 256
KN 76
KN 82
KN 84
KN 93
KN 95
HF131
HF126
HF111
MO 58
MO 79
MO 28
HF103
NAG39
NAG 41
NAG 43
NH39
HF141
NH40
NH 10
NH 8
NH 31
NAG 45
Pokhara
NAG 3
LO 312
Seti
Marsyandi
MO 107
LO 258
KN 102
MO 100
Gorkha
MO 125
Trisuli
Kathmandu
LO 316
LO 300
LO 314
LO 302
LO 304
Andhi
NH 7
LO 306
LO 308
Kali Gandaki
LO 310
Tansen
Nayarani
Alluvial deposits
Siwaliks
TSS
HHC
HHL
LH
LHN

Fig. 2a

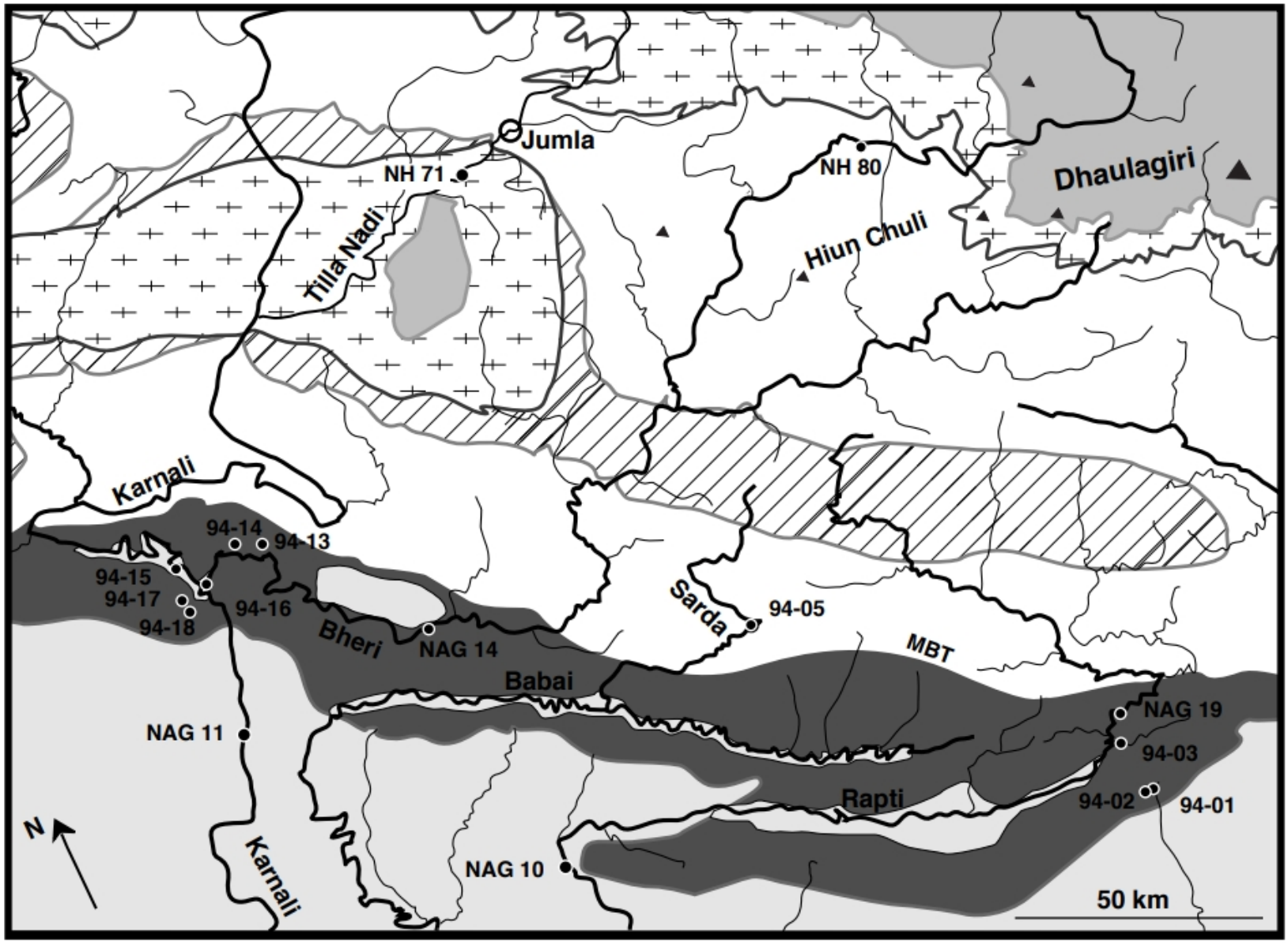
Jumla
NH 71
NH 80
Dhaulagiri
Tilla Nadi
Hiun Chuli
Karnali
94-14
94-13
94-15
94-17
94-18
94-16
Bheri
NAG 14
Sarda
94-05
MBT
Babai
NAG 19
94-03
NAG 11
Rapti
94-02
94-01
N
Karnali
NAG 10
50 km

Fig. 2b

Fig. 3a

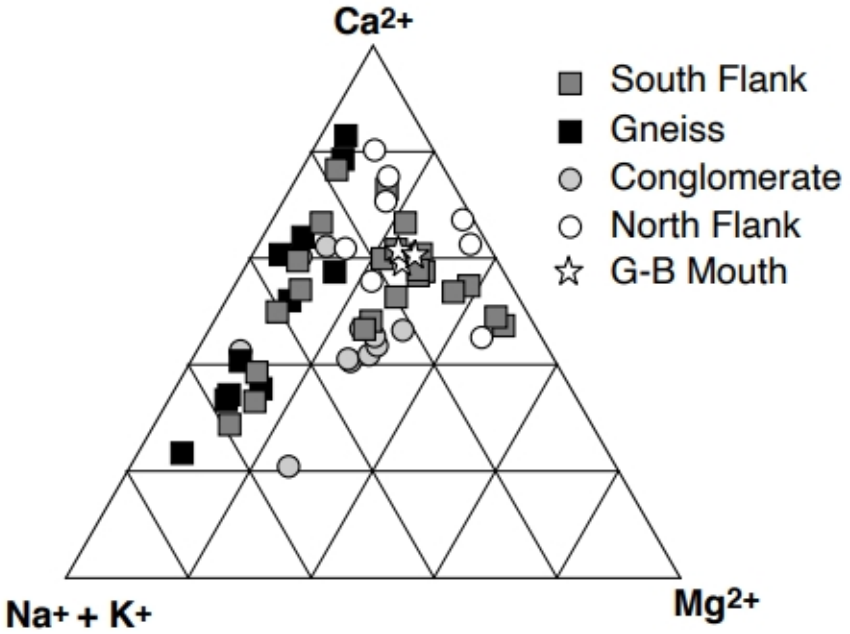
Ca2+
Na+ + K+
Mg2+
South Flank
Gneiss
Conglomerate
North Flank
G-B Mouth

Fig. 3b

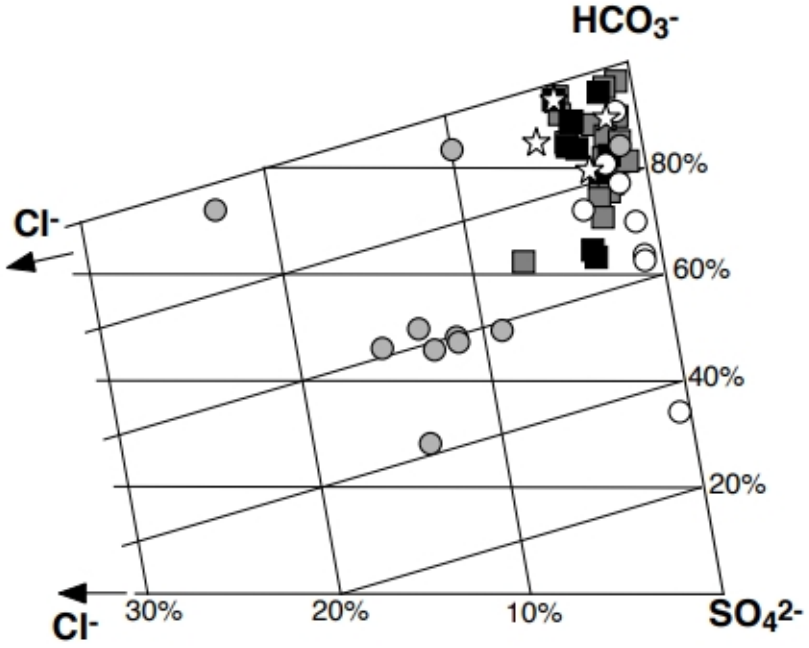
HCO3-
Cl-
80%
60%
40%
20%
Cl-
30%
20%
10%
SO4 2-

Fig. 4

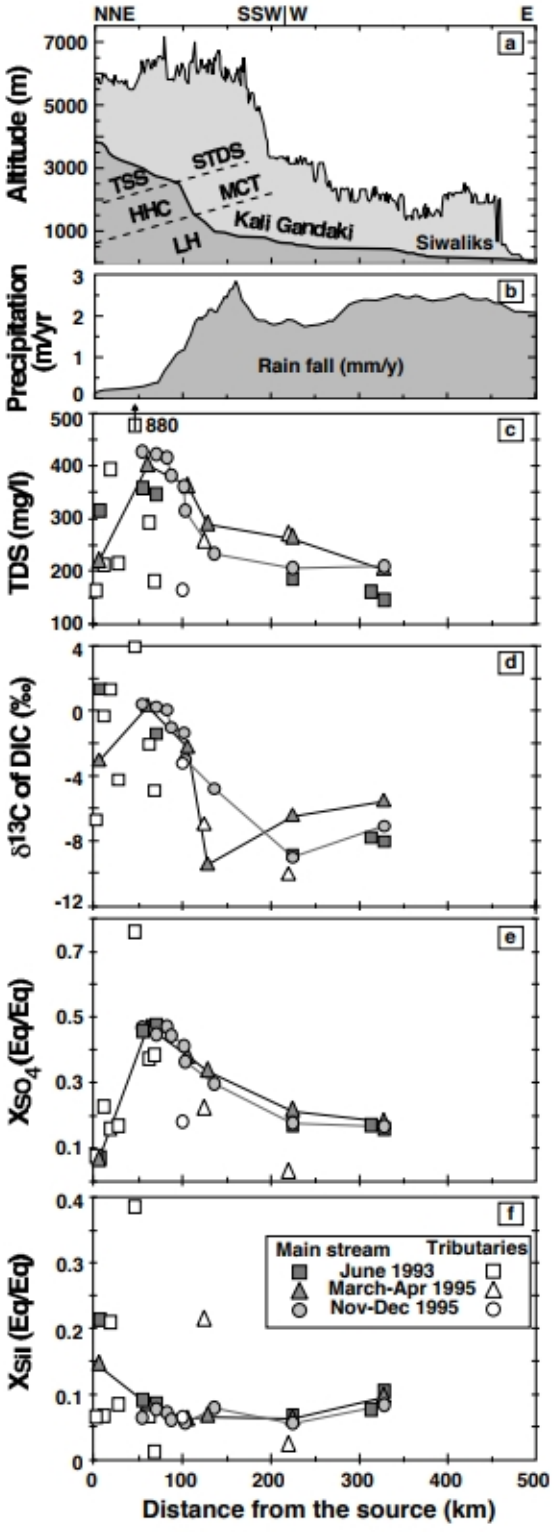
NNE
SSW|W
E
a
Altitude (m)
7000
5000
3000
1000
STDS
TSS
MCT
HHC
LH
Kali Gandaki
Siwaliks
b
Precipitation (m/yr)
3
2
1
0
Rain fall (mm/y)
c
880
TDS (mg/l)
500
400
300
200
100
d
δ13C of DIC (‰)
4
0
-4
-8
-12
e
XSO4 (Eq/Eq)
0.7
0.5
0.3
0.1
f
XSil (Eq/Eq)
0.4
0.3
0.2
0.1
0
Main stream
Tributaries
June 1993
March-Apr 1995
Nov-Dec 1995
0
100
200
300
400
500
Distance from the source (km)

Fig. 5

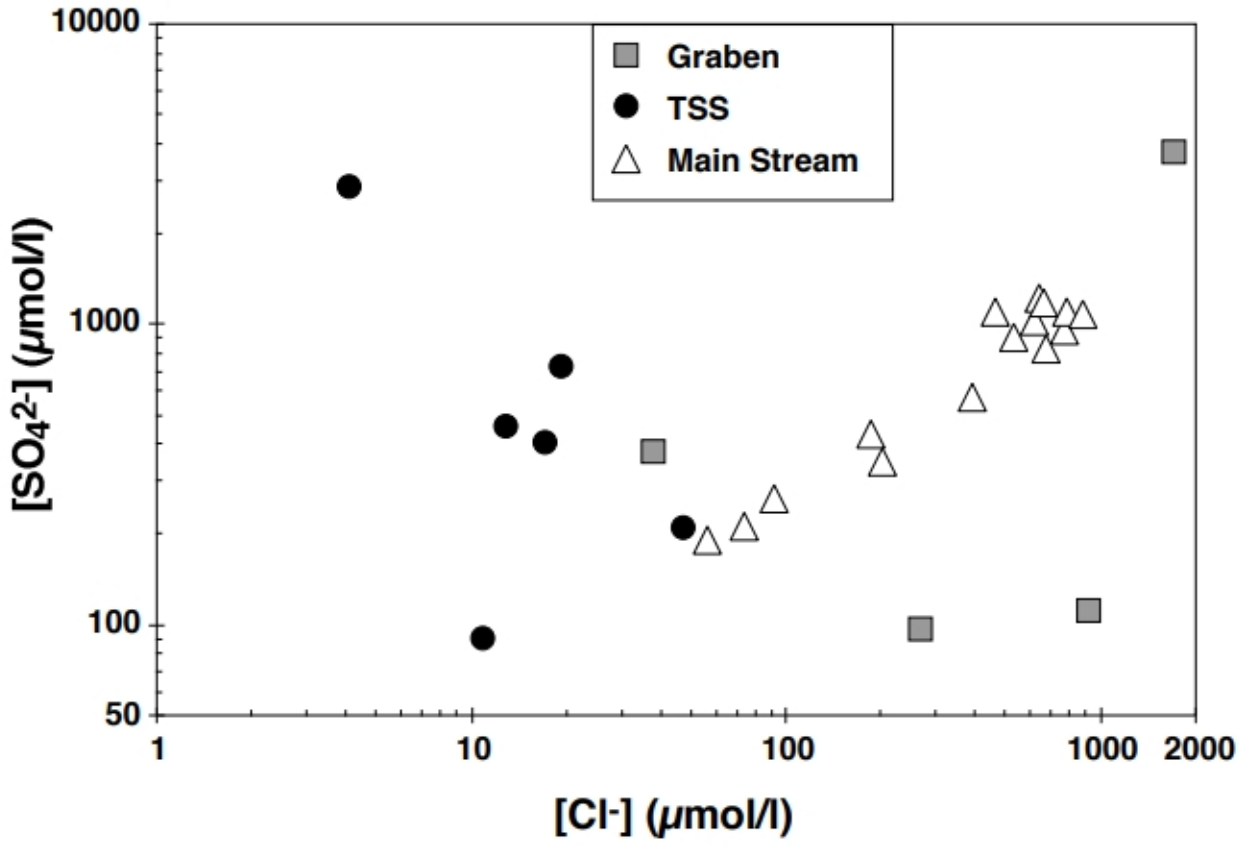
10000
1000
100
50
1
10
100
1000
2000
Graben
TSS
Main Stream
[SO4 2-] (µmol/l)
[Cl-] (µmol/l)

Fig. 6

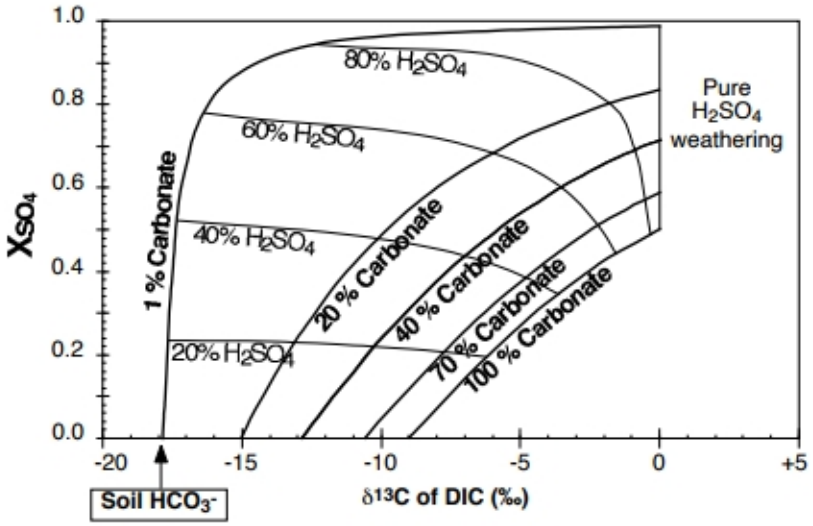

Fig. 6a

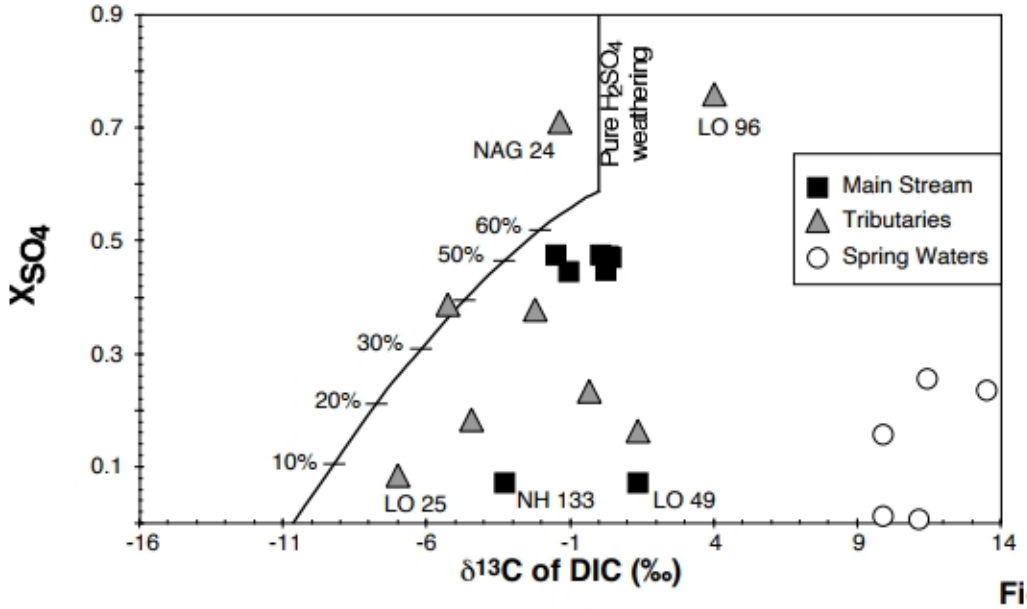

Fig. 6b

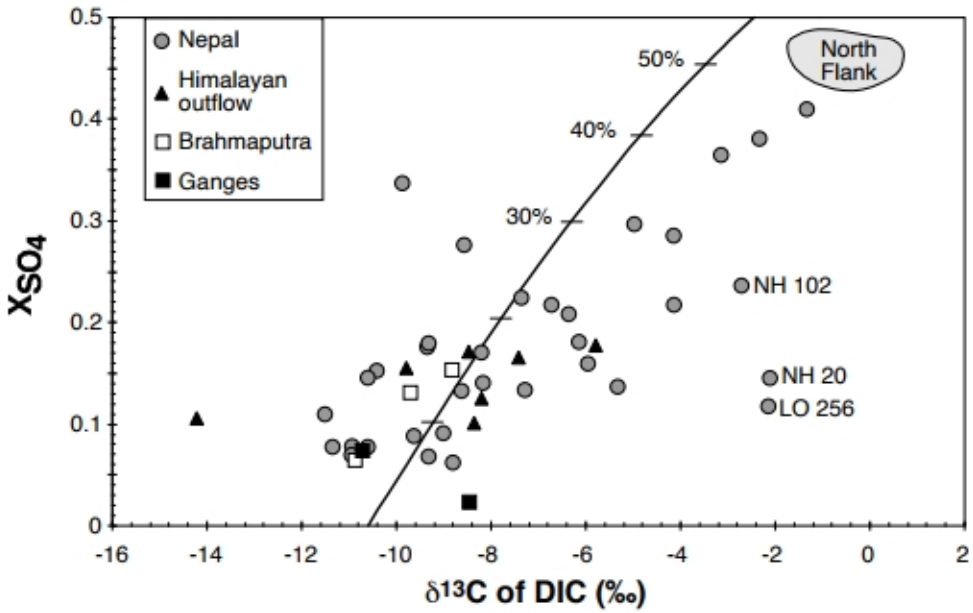

Fig. 7

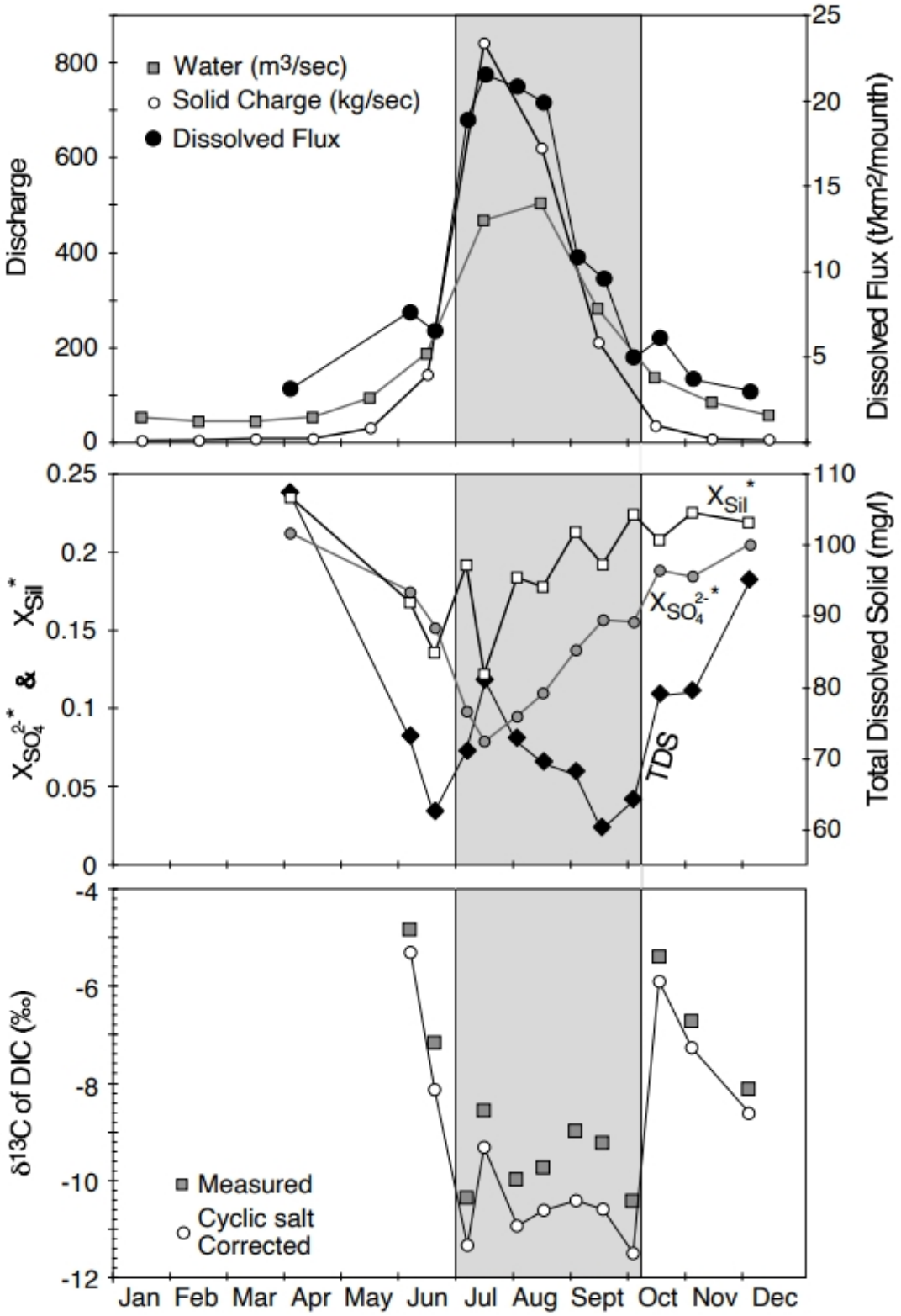
Water (m3/sec)
Solid Charge (kg/sec)
Dissolved Flux
Discharge
Dissolved Flux (t/km2/mounth)
800
600
400
200
0
25
20
15
10
5
0.25
0.2
0.15
0.1
0.05
0
110
100
90
80
70
60
XSil*
XSO4 2-*
TDS
XSO4 2-* & XSil*
Total Dissolved Solid (mg/l)
-4
-6
-8
-10
-12
δ13C of DIC (‰)
Measured
Cyclic salt Corrected
Jan Feb Mar Apr May Jun Jul Aug Sept Oct Nov Dec

Fig. 8

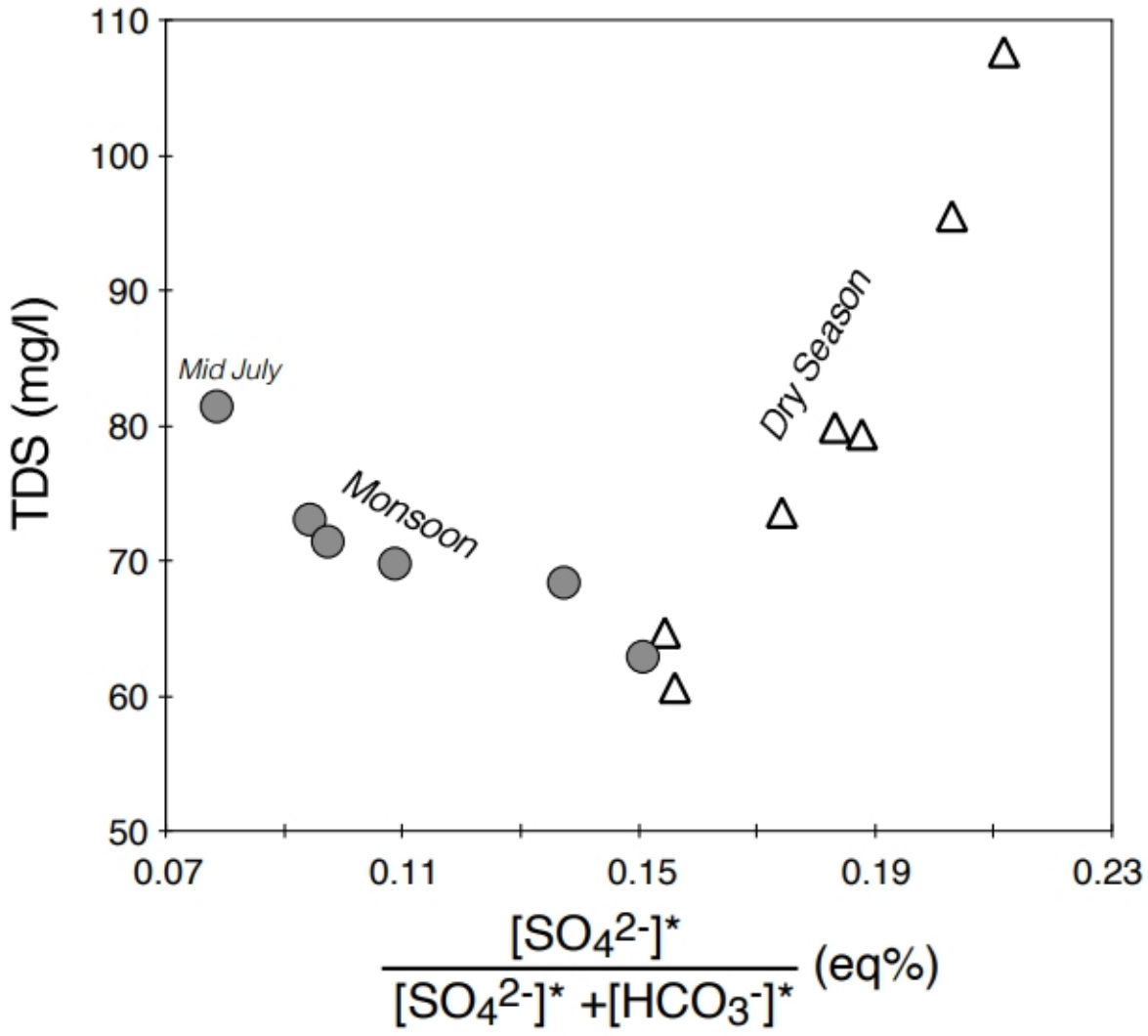
110
100
90
80
70
60
50
TDS (mg/l)
Mid July
Monsoon
Dry Season
0.07
0.11
0.15
0.19
0.23
$\frac{[SO_4^{2-}]^*}{[SO_4^{2-}]^* + [HCO_3^-]^*}$ (eq%)

Fig. 9

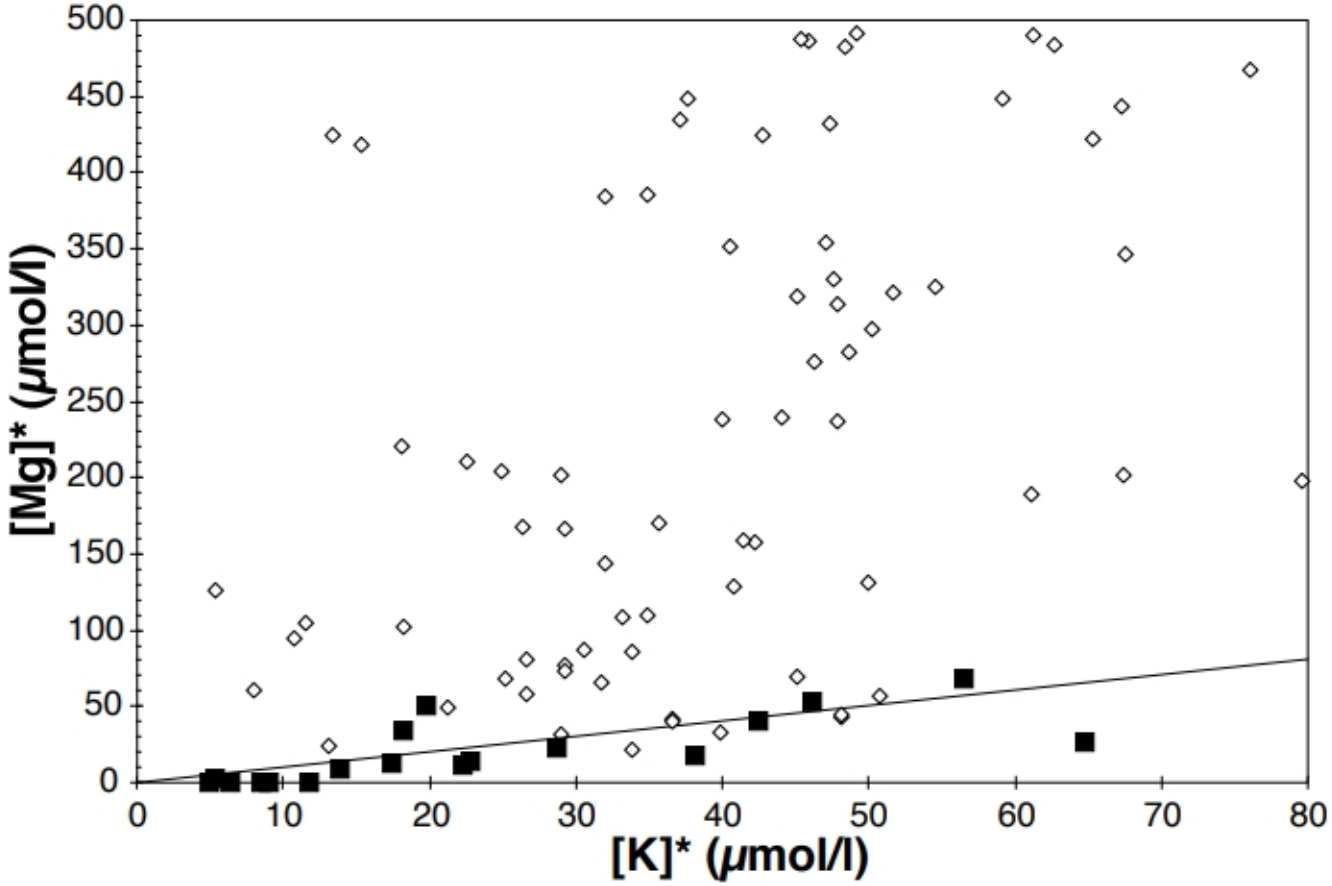
500
450
400
350
300
250
200
150
100
50
0
[Mg]* (µmol/l)
0
10
20
30
40
50
60
70
80
[K]* (µmol/l)